

LANDSAT SPECTRAL RESPONSES TO GRASSLAND BIOPHYSICAL  
CONDITIONS ACROSS A GRADIENT IN INNER MONGOLIA, CHINA

by

Jie Dai

A thesis submitted  
in partial fulfillment of the requirements  
for the degree of  
Master of Science  
(Natural Resources and Environment)  
in the University of Michigan  
April 2013

Thesis Committee:

Professor Daniel G. Brown, Chair

Associate Research Scientist Kathleen M. Bergen

## Abstract

To investigate the potential of using Landsat imagery to detect grassland biophysical conditions, in particular biomass and biodiversity, harvested aboveground biomass and biodiversity were recorded along an ecological gradient in Inner Mongolia Autonomous Region (IMAR), China. Simultaneously vegetation spectral signatures were recorded by an analytical spectral device (ASD) Fieldspec 3 spectrometer. Vegetation indices (VIs) were calculated from the field spectrometer data following the same method as that of traditional Landsat-derived indices. Spatial regression analysis was used to assess the relationships between biomass and biodiversity and VIs. Based on maximum log likelihood and Akaike's Information Criterion (AIC), we determined that the spatial error model between the log-transformations of both fresh biomass ( $\ln Biom\_f$ ) and RVI ( $\ln RVI$ ) ( $R^2=0.795$ ,  $\log = -13.77$ ,  $AIC = 31.54$ ) performed best in predicting fresh biomass for all sites. And the spatial error model between the log-transformations of both biodiversity ( $\ln Biod$ ) and RVI ( $\ln RVI$ ) ( $R^2=0.763$ ,  $\log = -0.70$ ,  $AIC = 5.40$ ) performed best in predicting biodiversity through the ecological gradients in the entire study area. When predicting dry biomass, the spatial error model between the log-transformations of both dry biomass ( $\ln Biom\_d$ ) and RVI ( $\ln RVI$ ) ( $R^2=0.662$ ,  $\log = -20.28$ ,  $AIC = 44.55$ ) was the best, but the estimations for dry biomass were generally poor. This study verifies that Landsat data can reasonably monitor grassland biophysical conditions across large areas and different ecoregions.

## Acknowledgements

I would like to thank Dr. Brown and Dr. Bergen for their assistance and guidance throughout this research, and my entire two years of master's study. I am very grateful to their patience and genuine support. I would also like to thank Mr. Shannon Brines and other ESA lab colleagues for their valuable help. Many thanks to the field survey team from the Institute of Botany, Chinese Academy of Sciences. Without their work I could never have finished this study. Last but not least, I would like to thank my parents, for supporting their son pursuing his dream at the other side of the Pacific Ocean. I can and will always feel your genuine love.

## Contents

Introduction .....	1
Study Area.....	6
Methods.....	8
Field data processing .....	8
Landsat imagery processing.....	9
Vegetation indices .....	10
Statistical analysis .....	12
Results.....	15
Detecting fresh biomass .....	15
Detecting dry biomass .....	16
Detecting biodiversity.....	17
Discussion.....	18
Conclusion.....	20
Figures and tables .....	21
Appendix: Regression reports for best-fit models.....	32
Citations .....	54

## Introduction

Covering about 40% of the global land area (Moore, 1966; Chapin et al., 2001), natural grasslands and savannas are undoubtedly among the most significant terrestrial ecosystems. They are also the dominant ecosystems in the vast semi-arid regions of the Eurasian continent (Sha et al. 2008). Unfortunately, due to global climate change, fast-growing human population and increasing grazing intensity, grassland degradation and desertification has been a great concern since the 1980s, especially in the Inner Mongolia Autonomous Region (IMAR), China (He et al., 2005; Kawamura et al., 2005). For example, over the past 50 years (1961-2010), the average grass productivity of IMAR has decreased from 1871 kg/ha to about 900 kg/ha, and nearly 90% of these grasslands are at various stages of degradation (Wang 2012). In order to promote grassland conservation and restoration, the accurate monitoring of aboveground grassland biophysical conditions - in particular biomass and biodiversity - is crucial.

Broadly speaking, biomass is the total mass of living matter (Ricklefs 2010). In this study, we concentrate on vegetation, or grass, within grassland areas of the Mongolian Plateau. There are two kinds of biomass for grass collected from the wild, namely fresh biomass and dry biomass. Fresh biomass (often also called wet biomass) is the mass of the fresh grass collected from the field. Fresh grass is dried in a heater at a certain temperature for certain length of time to make sure that all moisture is evaporated (Bai et al. 2008), and the weight of the remaining grass is the dry biomass. Because it includes the water content of plants, the amount of wet biomass is more responsive to changes in moisture conditions, driven by changes in the weather, whereas dry biomass is a measure of the amount photosynthetic activity carried out by annual plants over the period of a season and is less sensitive to recent weather.

Biodiversity refers to the variation among organisms and ecosystems, from the genetic variation within populations, morphological and functional differences among species, to

differences in biome structure and ecosystem process (Ricklefs 2010). In this study, we restrict our focus to biodiversity within grassland communities, measured as the number of species (i.e. species richness) occurring within the study area (Ricklefs 2010).

Biomass and biodiversity are both useful and important aspects of grassland ecosystem conditions. They are affected by climate change (Bai et al. 2008), and can be crucial parameters of terrestrial ecosystem process-based models (Ren et al. 2011). One way to monitor them is to conduct field surveys in the study area. Surveyors will usually record sample quadrat information on location, canopy structure, above-ground biomass, and the number and name of plant species (Bai et al. 2008). Although this traditional method can provide the most accurate vegetation information, it usually requires large amounts of sample quadrats, and is thus very time-consuming and expensive, especially when covering large areas (Xie et al., 2009).

In an effort to address these drawbacks, demand for applying remote sensing technology to grassland monitoring has been increasing because it can repeatedly monitor large scale with relatively lower costs. Remote sensing relies on spectral responses, and airborne and field spectrometer readings are a way of measuring spectral responses. Several works have shown the possibility and remarkable ability of using these spectrometers to detect grassland biomass and biodiversity (Mutanga 2004; Cho et al. 2007; Ren et al. 2011; Gao et al. 2012; and Rocchini 2007). Because of the chlorophyll and water in plants, healthy green vegetation has higher spectral reflectance in green wavelengths than in red, and a steep increase in reflectance in the near-infrared wavelengths. But for dry grass, the spectral reflectance will increase gently all the way from blue toward near-infrared wavelengths (Du et al. 2004). Spectral heterogeneity is more likely to occur in vegetation communities with higher level of diversity (Rocchini 2007; Palmer 2002). If spectral responses are sensitive to vegetation conditions and diversity, there is some

hope that satellite-imaging sensors can be used for estimating the same quantities. However, differences in sensor spectral and spatial resolution can reduce the sensitivity to vegetation conditions (Mutanga et al. 2004; Ren et al 2011). Mutanga et al. (2004) found out that when estimating the biomass of tropical grassland, narrow-band NDVI derived from spectrometer performed much better than standard NDVI ( $R^2 = 0.78$  vs.  $R^2 = 0.25$ ); the study of Ren et al. (2011) also showed that red-edge reflectance curve area method can better predict green aboveground biomass than traditional NDVI derived from Landsat in desert steppe.

Of the remote sensing satellites and sensors, the Landsat series of satellites has long served as effective tools for monitoring grassland dynamics throughout the world. The most widely used Landsat data is that collected by the multispectral sensors, Thematic Mapper (TM) on Landsat 4 and 5 and Enhanced Thematic Mapper Plus (ETM+) on Landsat 7. Using Landsat data, coupled with ground observations, can provide acceptable and affordable estimates of biomass and biodiversity (Li and Liu, 2001; Zheng *et al.*, 2004).

Statistical models have been used to build empirical relationships between Landsat-derived and other satellite-derived spectral data (using either original spectral bands or vegetation indices) and vegetation variables. There have been several efforts to build regression models to estimate grassland aboveground biomass using multispectral satellite data (Anderson et al., 1992; Schino et al. 2003; Xie et al. 2009). Anderson et al. (1992) developed bivariate models to examine the relationships between vegetation index (i.e., NDVI) derived from Landsat TM data and the aboveground biomass on semi-arid rangelands in northeast Colorado, USA. Although the results were not very satisfying due to sample size, they did reveal significant relationships between biomass and vegetation indices. Using refined ground campaigns carried out in previous years in central Italy, Schino et al. (2003) developed a simple linear regression function between

vegetation indices and the *in-situ* ground measurements. Indices that have been tested include NDVI and transformed soil adjusted vegetation index (TSAVI; Baret & Guyot 1991). They concluded that the NDVI provides better accurate estimate of grass biomass. Based on this idea, Xie et al. (2008) developed an artificial neural network (ANN) model to predicting biomass in the Xilingol River Basin in Inner Mongolia, China. They included spectral reflectance from Landsat Band 3 and 4, and reached a coefficient of determination of 0.817.

Landsat-derived spectral data have also been incorporated to predict or assess vegetation biodiversity for tropical trees (Gillespie et al. 2009), boreal plants (Gould 2000; Parviainen et al. 2009), and wetland marsh (Rocchini, D. 2007; Rocchini et al. 2007). The study of Gould (2000) show high correlation ( $r=0.808$ ) between NDVI and vascular plant species richness. Similarly, Rocchini (2007) found out that vegetation species richness was highly correlated to both Quickbird image heterogeneity ( $r=0.69$ ), and resampled 60 m Landsat ETM+ images ( $r=0.69$ ).

Although several studies have shown the possibility of using Landsat data to estimate grass biomass (Anderson et al., 1992; Schino et al. 2003; Xie et al. 2009) and biodiversity (Rocchini, D. 2007; Rocchini et al. 2007), as reviewed above, they were all taken in small areas or focused on one particular kind of grassland. To better monitor the grassland conditions in Inner Mongolia, China, the objective of this work is to investigate the responses of Landsat data to grassland fresh and dry biomass and species richness across an ecological gradient on the Mongolian plateau. I explore the possibility of estimating vegetation biomass and biodiversity by developing simple regression models. I first calculated vegetation indices (VI) measured by the spectrometer following the same method as that of Landsat, and their relationships to biomass/biodiversity. Then I relate biomass and biodiversity to VIs derived from Landsat imagery, and compare the predictive ability of Landsat and that of the spectrometer. Following this introduction, I briefly



introduce the study area and field data collection procedures. Then I illustrate the methods of processing the source data, as well as the statistical models applied for linking Landsat, in-situ hyperspectral data to the ecological data. The outcomes are presented in Results section. Finally, I will discuss the significance of the results, drawbacks of the analysis, and possible future improvements.

## Study Area

This study was conducted on the Mongolian Plateau in the Inner Mongolia Autonomous Region (IMAR) of China (Figure 1). Covering about 66% of the region's total land area, grasslands are the dominant ecosystem type of IMAR (Bai et al. 2008). In this study, 16 sites on the Mongolia Plateau were selected along a northeast-southwest transect, running from 41.86°-49.93° N latitude and 111.94°-120.42° E longitude. This transect covers mainly three vegetation community types. These are in order of their descending trend of annual precipitation: meadow steppe, typical steppe, and desert steppe. Geographically, they grade from northeast to southwest respectively. Most of the study area has a gentle ground slope with elevation ranging from about 600 m above sea level (ASL) in the northeast to 1500 m ASL in the southwest. The mean annual temperature (MAT) ranges from -1.5°C to 5.2°C, and mostly the further southwest, the warmer (Bai et al. 2008). However, the mean annual precipitation (MAP) presents a descending trend from northeast to southwest, ranging from about 180 to 500 mm (Bai et al. 2008). Approximately 70-80% of precipitation occurs in the growing season (May to August), synchronized with the warmer months of the year (Bai et al. 2008).

Within the study area, plant community types were found to have various levels of biomass, species richness, and MAP, the last of which is the major determinant of vegetation types. The meadow steppe in the northeast is mainly dominated by *Carex pediformis*, *Filifolium sibiricum*, *Stipa baicalensis*, *Stipa krylovii*, and *Leymus chinensis*. This vegetation community also has the highest biomass, species richness, and MAP. Dominated by *Leymus chinensis*, *Stipa grandis*, and *Anemarrhena asphodeloides*, the typical steppe shows intermediate levels of biomass, species richness, and MAP. Finally at the southwest end of the transect, the desert steppe is mostly dominated by *Artemisia frigida*, *Allium polyrhizum*, *Ceratoides latens*, *Salsola collinsa*, and *Stipa klemenzii*, and presents the lowest biomass, species richness, and MAP (Qi et al. 2008).



## Methods

### Field data processing

A field survey was conducted by a team from the Institute of Botany, Chinese Academy of Sciences, using a stratified sampling design during August, 2010. The sample sites were mainly adopted from Bai et al. (2008), and located with considerable respect to travel distance and availability. The data were collected at 16 sites, distributed among strata as follows: seven sites in meadow steppe, three in typical steppe, and six in desert steppe. For most of these sample sites, three replicate plots were sampled. The plot size was 90 m by 90 m, with approximately 50 m distance between each replicate. In meadow steppe, three of the six sites had permanent fences. For these three sites, six replicate plots were sampled: three located inside the enclosure, and three outside. In total, 57 field plots were sampled across the ecological gradients.

Nine 1 m by 1 m quadrats were sampled along the two diagonals within each square plot (Figure 2b). Within each quadrat, longitude/latitude (decimal degrees), canopy height (cm), canopy cover (%), above ground fresh biomass ( $\text{g/m}^2$ ), and the number and name of plant species (# and text), were measured. Later in the laboratory fresh grass was dried in a heater at 65°C for 48 hours to make sure that all moisture was evaporated (Bai et al. 2008). Then dry biomass ( $\text{g/m}^2$ ) was measured. A GPS device was used to measure the latitude and longitude at the quadrats and plot corners.

Meanwhile, 16 *in situ* canopy spectral samples, eight each along the two diagonals of each plot (Figure 2a), were recorded using Analytical Spectral Devices (ASD) FieldSpec 3 spectrometer. The spectrometer has a spectral range from 350 to 2500 nm with a sampling interval of 1.4 nm for spectrum 350-1000 nm and 2 nm for spectrum 1000-2500 nm. The sampled spectra were later interpolated by the ASD software to produce readings at every 1 nm (ASD Inc., Boulder, Colorado, USA).

The spectral samples were recorded between 10:00 am and 2:00 pm GMT +8 under sunny and clear weather conditions. With a 25° view angle, the sensor scanned from a 1.5 m height looking towards the nadir, thus the field of view (FOV) at the ground was 1.4 m in diameter. The equipment itself and any shadow were carefully avoided within the FOV. Each of the 16 replicates in one plot was automatically sampled ten times by the device. The sensor was calibrated with a white reference panel after every eight measurements to offset any variations in solar illuminations and weather conditions. The radiances recorded by the sensor were then converted to reflectance using the software package ViewSpecPro (ASD Inc., Boulder, Colorado, USA).

The converted reflectances were displayed in MATLAB (MathWorks Inc., Natick, Massachusetts, USA). First, measurements from the spectral range corresponding to the combined Landsat visible and infrared bands (Table 1) were kept and displayed (Figure 3). In the next step, outlier measurements were deleted and the remaining measurements taken at a given sample point were averaged to represent the spectral reflectance of that point. Then, all 16 replicates in one plot were averaged to represent the spectral reflectance of that plot (Figure 4). Finally, the measurements were averaged according to the spectral ranges of Landsat bands, so that we can calculate VIs from field spectrometer following the same method as that of Landsat-derived VIs.

### **Landsat imagery processing**

Five Landsat-5 TM scenes from 23 July to 5 September 2010 were acquired from USGS Earth Explorer (<http://glovis.usgs.gov/>) for this study. The processing levels are *terrain corrected processing*. The criteria for selection of imagery were:

- (1) No clouds or shadows should occur above the sampling sites.

(2) Scene date should be as close as possible to field sampling dates (Table 2), with respect to grassland phenology.

(3) Ideally, Landsat scenes and *in-situ* spectrometer should capture the spectral signatures of the grass in the same phase of growth, and under the same weather conditions.

The scenes were radiometrically and atmospherically corrected using ATCOR 3 module in ERDAS IMAGINE 2010. A digital elevation model (DEM) covering the study area with a spatial resolution of 30 m created from ASTER data was used in the atmospheric correction. All data were registered in a projected coordinate system based on the Albers Conical Equal Area projection.

To match the 90m by 90m ground sampling plots, the ArcGIS resample tool was used to create a 90m pixel size layer from the original 30m spatial resolution Landsat scene. For each sample plot, the processing extent was set to ensure that the plot's center overlapped the pixel's core, so that the entire plot was located within the same pixel (Figure 5). Both bilinear interpolation (BI) and cubic convolution (CC) were tested for resampling, and there was no apparent difference in the resulting digital number values. BI was used for resampling.

### **Vegetation indices**

Digital number values extracted from Landsat-5 TM bands 1, 2, 3, 4, 5 and 7 were used to compute the vegetation indices for input to the statistical analyses. The thermal infrared band (band 6) was not used in this study. Four vegetation indices were selected as potential predictive variables. These were the ratio vegetation index (RVI), NDVI, soil-adjusted vegetation index (SAVI) and modified soil-adjusted vegetation index (MSAVI).

RVI was reported in one study to have the highest correlation with sampled biomass (Ren 2008). It is produced by the following equation, where *NIR* is the Landsat near infrared band values (band 4) and *Red* is the red band values (band 3).

$$RVI = \frac{NIR}{Red}$$

Developed by Tucker (1979), NDVI is produced by the equation below. The NDVI reflects the degree of vegetation greenness on a scale between -1 and 1, with 1 being the greatest value. It was chosen because of its sensitivity to vegetation structure and productivity, and because it has been used to predict vegetation biomass for decades by many studies (Anderson et al., 1992; Schino et al. 2003; Mutanga 2004; Cho et al. 2007; Xie et al. 2009; and Gao et al. 2012).

$$NDVI = \frac{NIR - Red}{NIR + Red}$$

Since nearly one-half of the sampling plots (27 out of 57) are located in arid/semi-arid areas, the spectral reflectance from other land elements, especially soil, should be taken into consideration. Huete (1988, p. 295) developed SAVI to alleviate the influence of background soil brightness by incorporating a soil adjustment factor *L* and claimed it can “eliminate soil-induced variations in vegetation indices.” SAVI is calculated with the following equation.

$$SAVI = \frac{(1 + L)(NIR - Red)}{NIR + Red + L}$$

In this study, for each plot, the adjustment factor *L* was set to the average canopy coverage of the nine replicates.

Later Qi *et al.* (1994) argued that the soil adjustment factor *L* should vary in accordance with the amount of vegetation present, and replaced the constant with a variable function. This resulted in the modified SAVI, which is calculated with the equation below.

$$MSAVI = \frac{(2NIR + 1) - \sqrt{(2NIR + 1)^2 - 8(NIR - Red)}}{2}$$

### Statistical analysis

Simple linear regression analysis was used to analyze the relationships between each measure of grassland biophysical condition and each calculated vegetation index. The dependent variables were fresh biomass (*Biom\_f*) and dry biomass (*Biom\_d*), as well as biodiversity (*Biod*), which was represented by species richness, (i.e., the number of species occurred in the whole sampling plot). The independent variables were the four vegetation indices, RVI, NDVI, SAVI and MSAVI. Natural log transformations of above variables were also tested in the regression models.

Because plots within the same sampling site were relatively close to each other, the assumption of independence in the samples was likely violated, thus spatial autocorrelation was tested and taken into account. The most commonly used index for measuring spatial autocorrelation of residuals is Moran's I. The values of Moran's I fall in the range between -1 (indicating perfect dispersion) and 1 (perfect clustering), and a zero value indicates a totally random distribution.

There are two primary ways to deal with spatial autocorrelation in regression models. First, if the observed values of dependent variable values are directly influenced by the neighboring values, we can treat spatial correlation as a process or effect of interest, and add a "spatially lagged" dependent variable among the covariates (Anselin 1988; Ward & Gleditsch 2008). This is the spatial lag model, which is illustrated in the following equation:

$$y = \beta x + \rho W y + \varepsilon$$

where  $x$  is a matrix of observations on the independent variables,  $W y$  stands for the spatially lagged dependent variables for weights matrix  $W$ ,  $\rho$  is the spatial coefficient, and  $\varepsilon$  represents a vector of error terms.



Another way to address spatial issues is to use a spatial error model. The spatial error model is appropriate for situations where the dependent variable is not influenced by neighbors, but by some spatially clustered feature that is omitted from the model. Here we incorporate the spatial effects through an error term:

$$y = \beta x + \lambda W\varepsilon + \xi$$

where  $W\varepsilon$  stands for the vector of error terms, spatially weighted using the weights matrix  $W$ ;  $\lambda$  is the spatial error coefficient, and  $\xi$  is a vector of uncorrelated error terms.

The correlation coefficient ( $R^2$ ) is calculated based on the ratio between explained and unexplained (residual) variation, which requires the residuals to be independent from each other. The main reason we use spatial regression is that the residuals are not independent, thus the variances of parameter estimates are not accurately obtained. Because spatial regression requires a maximum likelihood estimator,  $R^2$  is no longer appropriate for stating and comparing fitness of the regression model. Instead, we will compare the *log likelihood* and *Akaike Information Criterion* (AIC) in the test report. *Log likelihood* is the measure for fit used by maximum-likelihood estimation (MLE) of the model. It provides estimates for the model parameters. In this case we would select the model with the highest *log likelihood*. Meanwhile AIC is a criterion for choosing the best one among a group of competing statistical models (Anselin 2005). We prefer the model with the lowest AIC.

Models were developed for all sites and, to analyze the effects of variations among ecoregion types, for only the meadow steppe sites. Meadow steppe sites was the only ecoregion for which we had sufficient observations (n=30) to perform an ecoregion-specific analysis.

The statistical analyses were performed in OpenGeoDa (Anselin 2012). For each pair of dependent and independent variables, I first perform a classic linear regression, and performed

diagnostics for spatial dependence in the residuals. If the test of the residual's Moran's I showed a significant result ( $p < 0.05$ ), which means spatial autocorrelation affected the results of the regression, a spatial lag model or spatial error model was implemented. The detailed model selection process can be found in Anselin (2005). In some instances, the model selection process was incomplete. These cases were usually due to heteroskedasticity of the variables, or misspecification of the model. Under these circumstances I dropped the particular relationship and use the either or both log-transformations of the original variables. In cases where none of the models with transformed variables produced results, the only method available was to discard this VI from the model.

## Results

The correlations between Landsat-derived and *in-situ* hyperspectral VIs fall in the range from 0.92 to 0.94 (RVI: 0.93, NDVI: 0.94, SAVI: 0.92, MSAVI: 0.93), which suggest a close and positive relationship. This close relationship implies that they have the potential to have similar predictive abilities.

The relationships between the dependent variables and the four selected VIs (i.e., RVI, NDVI, SAVI and MSAVI) show that both biomass and biodiversity had positive relationships with all VIs (Table 3 and 4). Reasonably strong relationships (i.e.,  $R^2 > 0.70$ ) were obtained for both biomass and biodiversity. The highest levels of predictive ability were generally observed for biomass, followed by biodiversity. Dry biomass consistently had the lowest levels of predictive ability (always  $R^2 < 0.70$ ).

### Detecting fresh biomass

Using VIs derived from field spectrometer, the models' coefficient of determination fell in the range 0.590 to 0.803 (Table 3). The spatial error model between the log-transformed fresh biomass  $\ln Biom\_f$  and NDVI ( $R^2=0.803$ ,  $\log = -9.44$ ,  $AIC = 22.88$ ) was best for the model with all 57 plots. For the 30 meadow plots, since the residual's Moran's I was not significant (Moran's I = 0.074,  $p=0.81$ ), the classic linear regression model was used. For this model, the models' coefficient of determination varied from 0.274 and 0.360. The log-transformations of both fresh biomass ( $\ln Biom\_f$ ) and NDVI ( $\ln NDVI$ ) resulted in the highest coefficient of determination ( $R^2=0.360$ ,  $p<0.001$ ).

As for the Landsat-derived VIs, the models' coefficient of determination fell in the range 0.684 to 0.795 (Table 4). The spatial error model between the log-transformations of both fresh biomass ( $\ln Biom\_f$ ) and RVI ( $\ln RVI$ ) ( $R^2=0.795$ ,  $\log = -13.77$ ,  $AIC = 31.54$ ) was the best in predicting fresh biomass for all plots. But for the meadow plots, because the Moran's I

calculated on the residuals was not significant (Moran's I = 0.038, p=0.49), the classic linear regression model was used. For this model, the models' coefficient of determination varied from 0.375 and 0.488. The log-transformations of both fresh biomass (*lnBiom\_f*) and NDVI (*lnNDVI*) presented the highest coefficient of determination ( $R^2=0.488$ ,  $p<0.001$ ). Field spectrometer data performed slightly better in predicting fresh biomass of all plots, but worse than Landsat in meadow plots.

### Detecting dry biomass

Using field spectrometer derived VIs, the models' coefficient of determination fell in the range 0.472 to 0.603 (Table 3). The spatial lag model between the log-transformed dry biomass *lnBiom\_d* and *MSAVI* ( $R^2=0.603$ ,  $\log = -23.98$ ,  $AIC = 53.96$ ) was best for the model with all 57 plots. For the 30 meadow plots, since the residual's Moran's I was not significant (Moran's I = 0.074, p=0.81), the classic linear regression model was used. For this model, the models' coefficient of determination varied from 0.155 and 0.173. Dry biomass (*Biom\_d*) and the log-transformation of NDVI (*lnNDVI*) presented the highest coefficient of determination ( $R^2=0.173$ , p=0.02).

As for the Landsat-derived VIs, the models' coefficient of determination fell in the range 0.467 to 0.662 (Table 4). The spatial error model between the log-transformations of both dry biomass (*lnBiom\_d*) and *RVI* (*lnRVI*) ( $R^2=0.662$ ,  $\log = -20.28$ ,  $AIC = 44.55$ ) was the best in predicting fresh biomass for all plots. But for the meadow plots, because the Moran's I calculated on the residuals was not significant (Moran's I = 0.038, p=0.49), the classic linear regression model was used. For this model, the models' coefficient of determination varied from 0.261 and 0.326. The log-transformations of both dry biomass (*lnBiom\_d*) and NDVI (*lnNDVI*)

presented the highest coefficient of determination ( $R^2=0.326$ ,  $p<0.01$ ). Landsat performed better in predicting dry biomass of both all plots and meadow plots.

### **Detecting biodiversity**

When using field spectrometer derived VIs, the models' coefficient of determination fell in the range 0.696 to 0.719 (Table 5). The spatial lag model between the log-transformations of *lnBiod* and *MSAVI* performed the best in predicting species richness for both all plots ( $R^2=0.719$ ,  $\log = -4.82$ ,  $AIC = 15.64$ ). For meadow plots, the models' coefficient of determination varied from 0.341 and 0.472. The spatial error model between *lnBiod* and *MSAVI* ( $R^2=0.472$ ,  $\log = -0.22$ ,  $AIC = 4.44$ ) was the best.

When using Landsat-derived VIs, the models' coefficient of determination fell in the range 0.717 to 0.763 (Table 6). The spatial error model between the log-transformations of both biodiversity (*lnBiod*) and RVI (*lnRVI*) ( $R^2=0.763$ ,  $\log = -0.70$ ,  $AIC = 5.40$ ) performed best for all plots. For meadow plots, the models' coefficient of determination falls in the range between 0.472 and 0.680. The spatial error model between *lnBiod* and *MSAVI* ( $R^2=0.680$ ,  $\log = 5.44$ ,  $AIC = -6.88$ ) was superior for meadow plots. Landsat performed better in estimating biodiversity for both all plots and meadow plots.

## Discussion

The predictive ability of the VIs for fresh biomass was consistently better than that of dry biomass. This may suggest that instead of providing precise quantities about the amount of vegetation productivity over a season, and serving as an adequate substitute for ecological measurements, remote sensing is more capable of monitoring ecosystem conditions that change over a short time period. The sensitivity of fresh biomass to moisture conditions, for example, suggest that remote sensing can be used, and has been used, to monitor drought conditions in grasslands.

When predicting fresh aboveground biomass, the field spectrometer data performed slightly better than Landsat for all sites across the ecological gradients. Due to the atmospheric effects that affect the Landsat measurements, but not those that come from the spectrometer, this result is as what I expected. However, that they both present reasonable potentials of predicting grassland biomass holds promise for the use of satellite sensors for measuring grassland condition.

Models predicting all plots always performed better than for meadow plots. A possible reason may be the sample size and reduced variability of a single eco-region. Since we are not including the full variability between desert, typical and meadow steppe, meadow steppe is undoubtedly less diverse than the full set of sites; thus we may get poorer fit of the models.

As for species richness, Landsat-derived VIs had a better predictive ability than the spectrometer-derived VIs. According to the Spectral Variation Hypothesis (Palmer, 2002), the foundation for satellite images to predict plant species richness is to capture the spectral differences of different plants. The reason Landsat-derived VIs performed better is likely due to the greater spectral variation being encompassed as Landsat sensors captured the spectral reflectance of the whole plot, whereas the spectrometer covering only 16 sample points with a

1.4-meter-diameter FOV. What's more, the trimming and averaging of the spectral details captured by the spectrometer can result in significant losses of information, where continuous quantitative spectral reflectance was degraded into discrete bands. Using more of the information in the spectrometer signatures could surely improve the predictive ability of these data. The crucial point is to detect the potential spectral heterogeneity between different plant species.

As for the drawbacks of this study, possible variations may come from the different dates between Landsat imagery and field survey (Table 2). I tried to ensure the dates were as close as possible and in the same grass phenological stage, but there were still inevitably gaps of 6 to 17 days. What's more, some of the models could not be estimated for some reason. This is not implausible because the variables were not independent. We substituted variables with their log-transformed versions in attempt to fit the models. But there are still cases where we cannot use one particular VI to predict dependent variables. For example none of the Landsat-derived SAVI models can pass the spatial model selection process. Unfortunately, this makes a complete comparison of the predictability of each VIs for each ecological variable impossible.

## Conclusion

- (1) The poor fitness of the dry biomass models indicates that VIs (both Landsat- derived and field spectrometer-derived) are not good indicators for the variable.
- (2) Landsat can decently reflect grassland biophysical conditions through gradients in Inner Mongolia, China. Landsat-derived RVI is best for estimating both fresh biomass and biodiversity through the gradients. The spatial error model between the log-transformations of both fresh biomass ( $\ln Biom\_f$ ) and RVI ( $\ln RVI$ ) performed best in predicting fresh biomass for all sites. And the spatial error model between the log-transformations of both biodiversity ( $\ln Biod$ ) and RVI ( $\ln RVI$ ) performed best in predicting biodiversity through the ecological gradients.
- (3) VIs calculated from field spectrometer data following the traditional Landsat method performed slightly better in predicting fresh biomass than Landsat-derived VIs. But the latter work better in predicting biodiversity.
- (4) Instead of serving as an adequate substitute for ecological productivity measurements, remote sensing is more suitable for monitoring ecosystem conditions.
- (5) Limitations in the spatial-statistical modeling approach resulting from models that did not converge meant that the exploration and comparison of VIs for predicting ecological variables was incomplete.



## Figures and tables

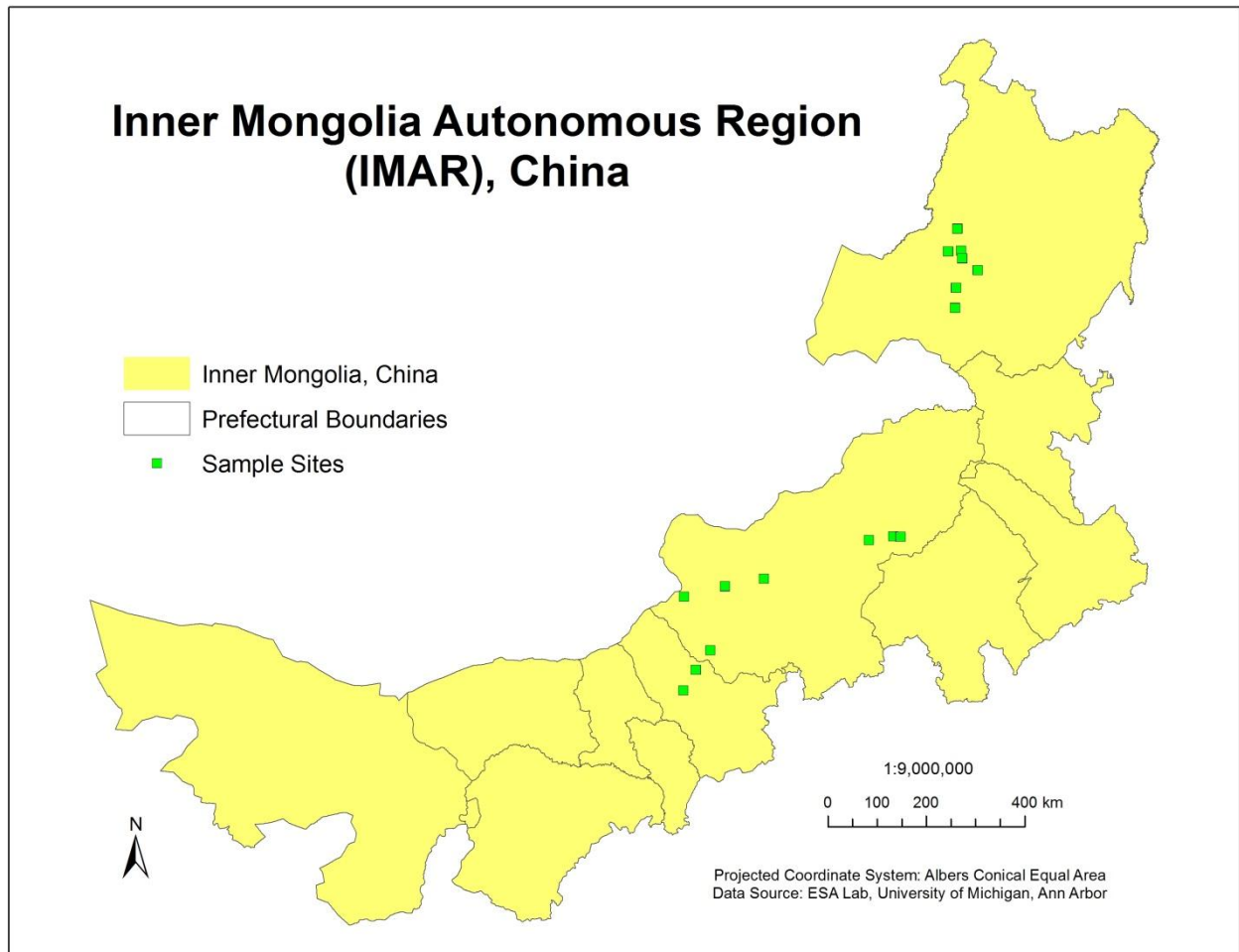


Figure 1: Study area and sample sites.

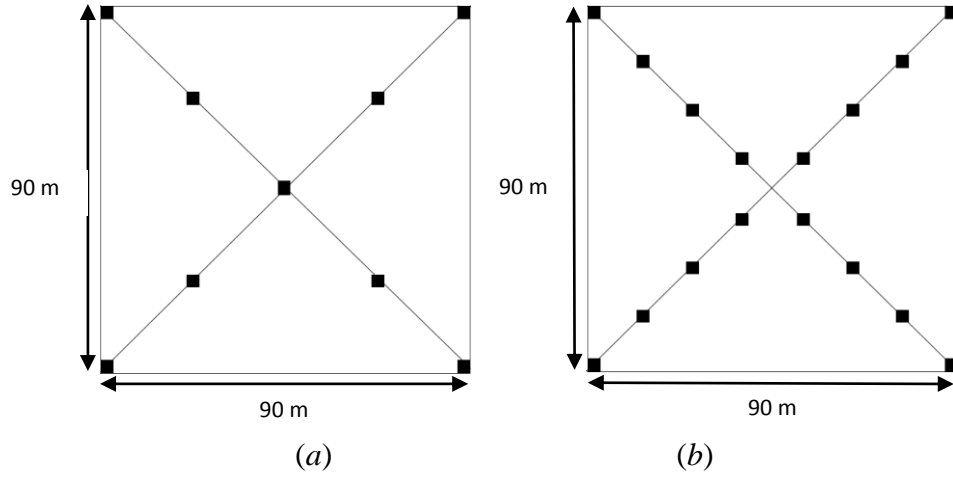
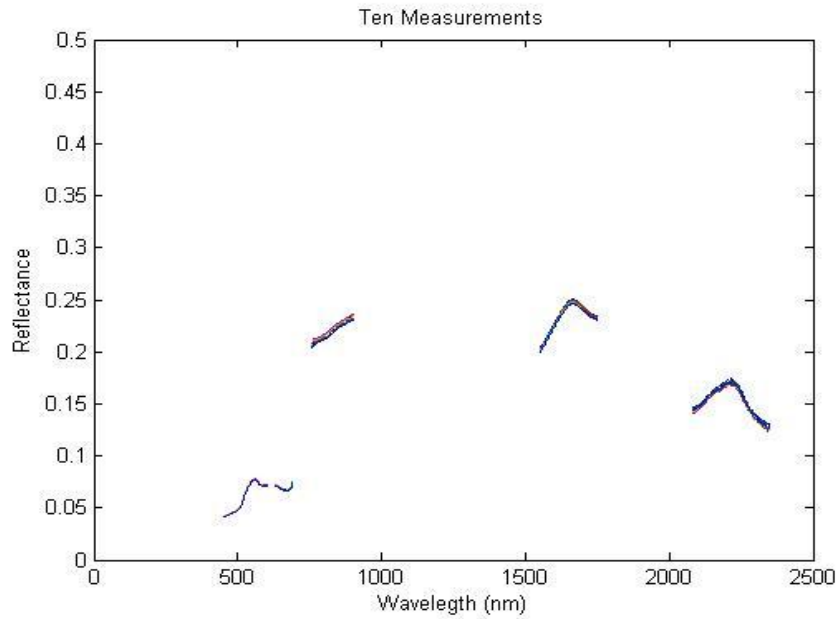
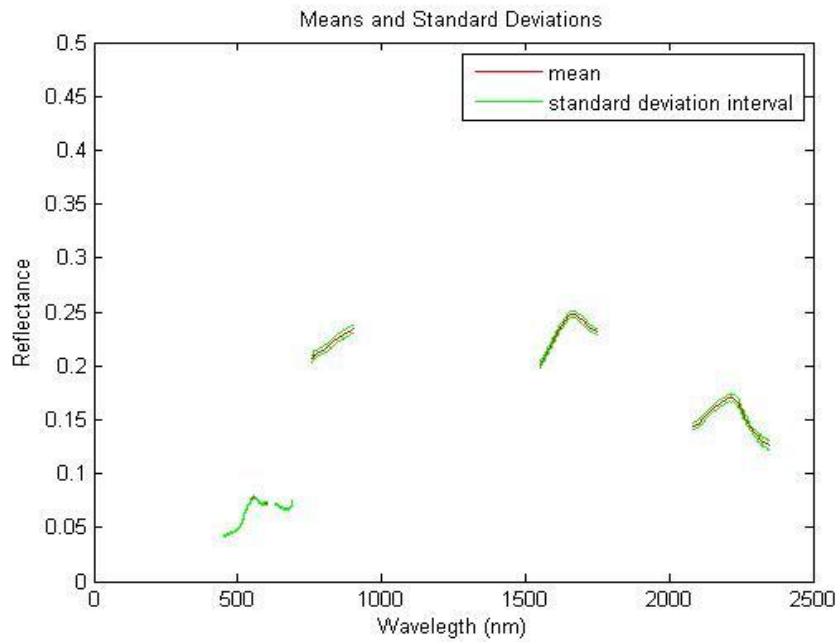


Figure 2: Spatial distributions of hyperspectral sampling points and ecological sampling quadrats in each field plot: (a) sampling patterns for ecological data; (b) sampling patterns for hyperspectral data.

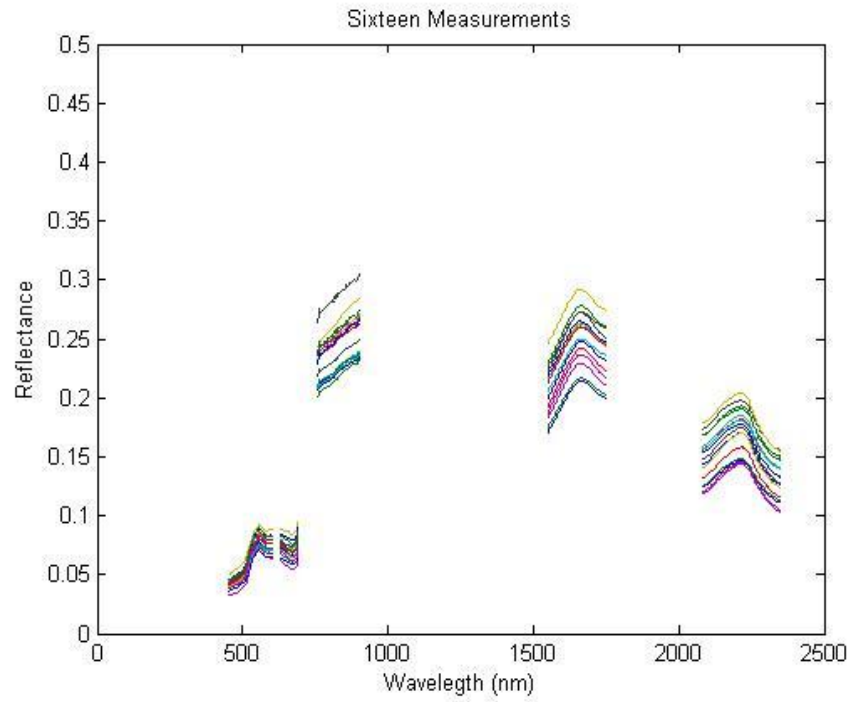


(a)

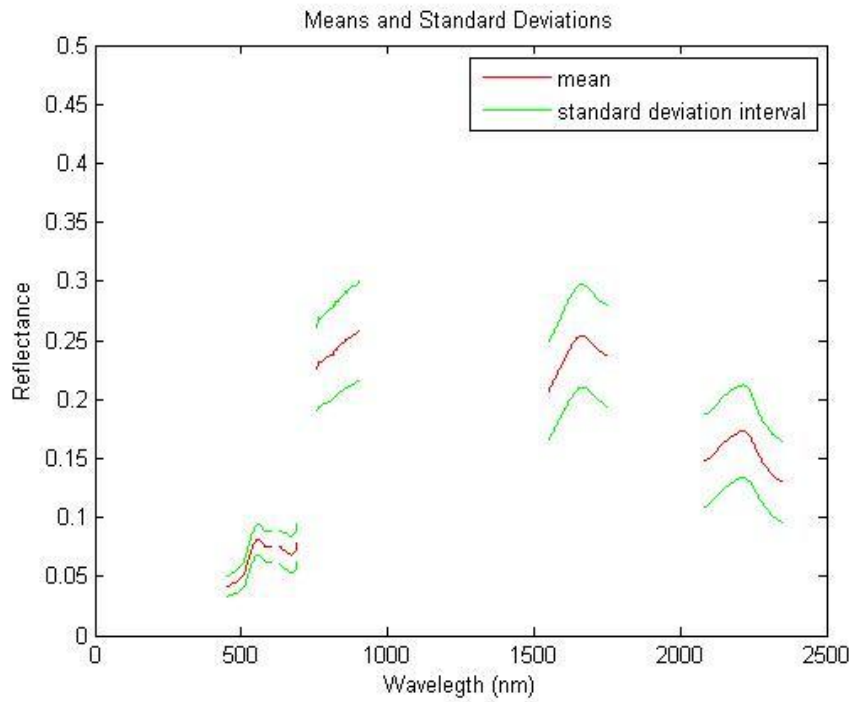


(b)

Figure 3: Spectrum corresponds to Landsat bands were kept while other parts of the spectrum were disposed. (a) ten measurements of one replicate; (b) mean and standard deviation interval of the ten measurements.



(a)



(b)

Figure 4: Sixteen replicates in one plot were averaged to represent the spectral reflectance of that plot. (a) sixteen replicates of one plot; (b) mean and standard deviation interval of the sixteen measurements.

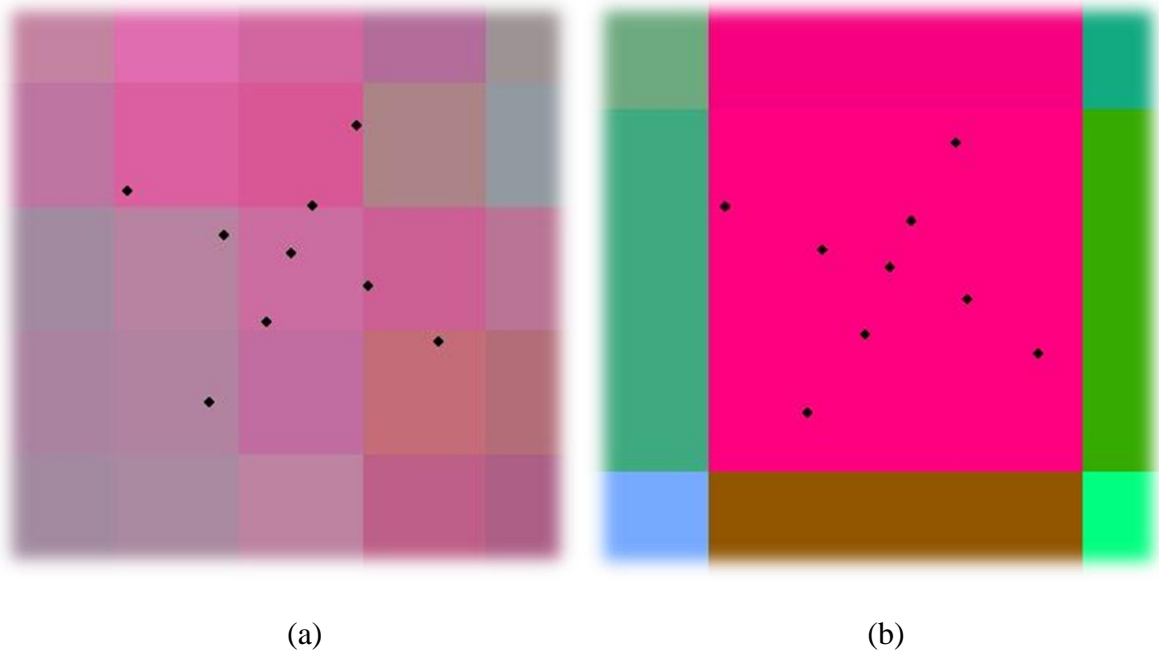


Figure 5: Landsat imagery was resampled from the original 30 m spatial resolution (a) to 90 m-by-90 m-pixel layers (b). For each sampling plot, processing extent was set to ensure that the plot's center would overlap the pixel's core, so that the entire plot would locate within the same pixel.

Table 1: Landsat Bands

Landsat Band	Spectrum (nm)	
1	450-520	Blue
2	520-600	Green
3	630-690	Red
4	760-900	Near-Infrared (NIR)
5	1550-1750	Mid-Infrared (MIR)
7	2080-2350	Mid-Infrared (MIR)

Table 2: Ground sampling dates and corresponding Landsat scene dates

Type	Site	Hyper Date	Landsat Scene Path/Row	Landsat Date
Meadow	1	30 Jul	123/026	23 Jul
	2	31 Jul		
	3	2 Aug	123/025	
	4	4 Aug	123/026	
	5	5/6 Aug		
	6	7 Aug		
	7	8/9 Aug		
Typical	8	14 Aug	123/029	24 Aug
	9	15 Aug		
	10	15 Aug		
Desert	11	19 Aug	126/030	13 Aug
	12	19 Aug		
	13	21 Aug		
	14	21 Aug		
	15	25 Aug	127/031	5 Sep
	16	25 Aug		

Table 3: Coefficient of determination ( $R^2$ ), maximum log likelihood and Akaike's Information Criterion (AIC), and estimated coefficients for the relationships between fresh and dry-aboveground biomass and spectrometer-derived VIs. Bold numbers stand for best fit models; N stands for non-significant results ( $p < 0.05$ ); \* implies incomplete model selection process and spatial regression models cannot be implemented.

Indices	Biomass ~ Spectrometer VIs															
	All										Meadow					
	Fresh					Dry					Fresh			Dry		
	$R^2$	slope	intercept	log	AIC	$R^2$	slope	intercept	log	AIC	$R^2$	slope	intercept	$R^2$	slope	intercept
	Biom ~ VI															
RVI			*					*			0.274	12.84	58.18	0.155	4.28	36.68
NDVI			*					*			0.325	276.23	-53.54	<b>0.173</b>	<b>89.61</b>	<b>1.00</b>
SAVI	0.590	130.53	-1.45	-282.1	570.355	0.472	51.49	5.33	-243.4	492.714		N			N	
MSAVI	0.613	158.39	-1.35	-278.0	565.992	0.489	59.99	5.54	-242.2	490.393		N			N	
	Biom ~ lnVI															
RVI			*					*			0.311	74.86	6.82	0.169	24.54	20.20
NDVI			*					*			0.328	175.28	203.46	0.173	56.50	84.20
SAVI	0.590	36.43	87.12	-281.9	569.757	0.478	15.19	41.84	-242.8	491.612		N			N	
MSAVI			*					*				N			N	
	lnBiom ~ VI															
RVI	0.749	0.10	1.09	-18.49	42.974			*			0.303	0.11	4.18	0.157	0.08	3.57
NDVI	<b>0.803</b>	<b>2.72</b>	<b>3.08</b>	<b>-9.440</b>	<b>22.881</b>			*			0.357	2.40	3.21	0.165	1.71	2.90
SAVI	0.730	1.74	1.05	-20.14	46.273	0.589	1.38	1.07	-25.15	56.308		N			N	
MSAVI	0.746	1.91	1.14	-18.12	42.245	<b>0.603</b>	<b>1.51</b>	<b>1.12</b>	<b>-23.98</b>	<b>53.956</b>		N			N	
	lnBiom ~ lnVI															
RVI			*					*			0.343	0.65	3.73	0.166	0.47	3.26
NDVI	0.797	0.97	5.22	-9.505	23.011			*			<b>0.360</b>	<b>1.52</b>	<b>5.44</b>	0.161	1.06	4.48
SAVI	0.740	0.56	2.65	-18.14	42.283	0.595	0.41	2.16	-24.30	54.602		N			N	
MSAVI	0.762	0.61	3.04	-15.06	36.127			*				N			N	



Table 4: Coefficient of determination ( $R^2$ ), maximum log likelihood and Akaike's Information Criterion (AIC), and estimated coefficients for the relationships between fresh and dry-aboveground biomass and Landsat-derived VIs. Bold numbers stand for best fit models; N stands for non-significant results ( $p < 0.05$ ); \* implies incomplete model selection process and spatial regression models cannot be implemented.

Indices	Biomass ~ Landsat VIs															
	All										Meadow					
	Fresh					Dry					Fresh			Dry		
	$R^2$	slope	intercept	log	AIC	$R^2$	slope	intercept	log	AIC	$R^2$	slope	intercept	$R^2$	slope	intercept
	Biom ~ VI															
RVI	0.728	20.02	26.35	-272.1	548.240	0.603	8.17	18.26	-236.1	476.291	0.375	18.54	28.35	0.261	6.88	23.25
NDVI	0.684	208.51	-2.94	-275.0	554.050			*			0.421	388.60	-130.59	0.299	145.48	-36.58
SAVI			*					*			N			N		
MSAVI			*					*			N			N		
	Biom ~ lnVI															
RVI	0.712	79.19	8.98	-273.0	549.927	0.590	31.61	11.93	-236.5	476.975	0.406	104.16	-42.23	0.286	38.82	-3.23
NDVI			*					*			0.429	255.50	233.87	0.307	96.12	100.07
SAVI			*			0.467	13.96	37.24	-244.0	494.092		N			N	
MSAVI			*					*			N			N		
	lnBiom ~ VI															
RVI	0.792	0.20	3.70	-15.24	34.473	0.667	0.18	3.08	-20.53	45.065	0.413	0.16	3.92	0.271	0.14	3.30
NDVI	0.783	2.49	3.22	-14.63	33.257			*			0.477	3.43	2.51	0.316	2.91	2.09
SAVI	0.712	1.48	0.82	-23.01	52.022	0.573	1.12	0.91	-27.07	60.138		N			N	
MSAVI			*					*				N			N	
	lnBiom ~ lnVI															
RVI	<b>0.795</b>	<b>0.89</b>	<b>3.42</b>	<b>-13.77</b>	<b>31.537</b>	<b>0.662</b>	<b>0.74</b>	<b>2.90</b>	<b>-20.28</b>	<b>44.554</b>	0.455	0.91	3.29	0.300	0.77	2.77
NDVI			*					*			<b>0.488</b>	<b>2.26</b>	<b>5.72</b>	<b>0.326</b>	<b>1.93</b>	<b>4.83</b>
SAVI	0.715	0.46	1.98	-22.28	50.566	0.574	0.33	1.71	-26.84	59.670		N			N	
MSAVI			*					*				N			N	

Table 5: Significant coefficient of determination ( $R^2$ ), maximum log likelihood and Akaike's Info Criterion (AIC) for the relationships between biodiversity and spectrometer-derived VIs. Bold numbers stand for best fit models; \* implies incomplete model selection process and spatial regression models can't be implemented.

Indices	Biodiversity ~ Hyperspectral VIs									
	All					Meadow				
	R <sup>2</sup>	slope	intersect	log	AIC	R <sup>2</sup>	slope	intersect	log	AIC
	Biod ~ VI									
RVI						0.396	3.98	18.57	-107.47	218.947
NDVI	0.696	49.24	3.90	-196.09	396.182	0.436	87.78	-17.76	-106.79	217.578
SAVI			*					*		
MSAVI			*			0.500	84.47	6.62	-104.50	213.000
	Biod ~ lnVI									
RVI	0.708	17.69	7.73	-194.81	393.621	0.443	24.03	1.24	-106.56	217.123
NDVI			*			0.403	53.68	62.86	-107.53	219.052
SAVI			*					*		
MSAVI			*			0.511	33.08	71.73	-104.21	212.422
	lnBiod ~ VI									
RVI	0.706	0.08	0.90	-7.087	20.174	0.394	0.12	3.02	-2.520	9.039
NDVI			*			0.382	2.44	2.05	-2.883	9.765
SAVI	0.711	1.74	0.99	-5.507	17.013	0.392	2.38	2.63	-1.675	7.351
MSAVI	<b>0.719</b>	<b>1.69</b>	<b>0.99</b>	<b>-4.821</b>	<b>15.641</b>	<b>0.472</b>	<b>2.45</b>	<b>2.69</b>	<b>-0.221</b>	<b>4.443</b>
	lnBiod ~ lnVI									
RVI			*			0.409	0.68	2.55	-2.284	8.567
NDVI			*			0.341	1.46	4.27	-3.688	11.377
SAVI			*			0.387	0.94	4.47	-1.752	7.505
MSAVI			*			0.468	0.94	4.56	-0.285	4.570

Table 6: Significant coefficient of determination ( $R^2$ ), maximum log likelihood and Akaike's Info Criterion (AIC) for the relationships between biodiversity and Landsat-derived VIs. Bold numbers stand for best fit models; \* implies incomplete model selection process and spatial regression models can't be implemented.

Indices	Biodiversity ~ Landsat VIs									
	All					Meadow				
	R <sup>2</sup>	slope	intersect	log	AIC	R <sup>2</sup>	slope	intersect	log	AIC
	Biod ~ VI									
RVI	0.761	5.29	8.91	-188.83	381.650	0.602	5.96	9.69	-102.23	208.452
NDVI	0.717	54.00	1.79	-193.17	390.333	0.566	117.64	-36.28	-103.39	210.770
SAVI			*			0.591	146.20	-17.75	-101.38	206.753
MSAVI			*			0.719	134.01	-6.11	-97.823	199.647
Biod ~ lnVI										
RVI	0.745	20.42	4.88	-190.28	384.557	0.598	32.78	-11.43	-102.42	208.841
NDVI			*			0.529	74.00	72.30	-104.36	212.727
SAVI			*			0.557	52.36	89.07	-102.36	208.711
MSAVI			*			0.680	47.43	91.63	-99.455	202.909
lnBiod ~ VI										
RVI	0.767	0.17	2.60	-1.184	6.369	0.579	0.17	2.78	2.027	-0.054
NDVI	0.746	1.94	2.28	-2.320	8.641	0.514	3.34	1.49	0.218	3.564
SAVI			*			0.554	4.23	1.99	2.454	-0.908
MSAVI			*			<b>0.680</b>	<b>3.89</b>	<b>2.33</b>	<b>5.442</b>	<b>-6.884</b>
lnBiod ~ lnVI										
RVI	<b>0.763</b>	<b>0.71</b>	<b>2.42</b>	<b>-0.700</b>	<b>5.399</b>	0.557	0.94	2.18	1.345	1.309
NDVI			*			0.472	2.08	4.56	-0.755	5.511
SAVI			*			0.521	1.51	5.07	1.622	0.756
MSAVI			*			0.629	1.36	5.14	3.619	-3.239

## Appendix: Regression reports for best-fit models

Classic linear regression between *lnBiom<sub>f</sub>* and Landsat derived *lnRVI* for all sites.

```

Regression
SUMMARY OF OUTPUT: ORDINARY LEAST SQUARES ESTIMATION
Data set      : landsat_thies
Dependent variable : lnBiom_f   Number of Observations: 57
Mean dependent var : 4.39947   Number of Variables : 2
S.D. dependent var : 0.626251  Degrees of Freedom : 55

R-squared      : 0.602142  F-statistic      : 83.2402
Adjusted R-squared : 0.594908  Prob(F-statistic) :1.34142e-012
Sum squared residual: 8.89405   Log likelihood   : -27.9359
Sigma-square    : 0.16171  Akaike info criterion : 59.8719
S.E. of regression : 0.402132  Schwarz criterion : 63.958
Sigma-square ML  : 0.156036
S.E. of regression ML: 0.395014
    
```

Variable	Coefficient	Std. Error	t-Statistic	Probability
CONSTANT	3.372561	0.1245218	27.08411	0.0000000
LNR	0.9039015	0.09907283	9.123607	0.0000000

```

REGRESSION DIAGNOSTICS
MULTICOLLINEARITY CONDITION NUMBER 4.451007
TEST ON NORMALITY OF ERRORS
TEST      DF      VALUE      PROB
Jarque-Bera      2      3.402941  0.1824151
    
```

```

DIAGNOSTICS FOR HETEROSKEDASTICITY
RANDOM COEFFICIENTS
TEST      DF      VALUE      PROB
Breusch-Pagan test      1      5.392794  0.0202201
Koenker-Bassett test    1      8.115459  0.0043889
SPECIFICATION ROBUST TEST
TEST      DF      VALUE      PROB
white      2      8.115789  0.0172854
    
```

```

DIAGNOSTICS FOR SPATIAL DEPENDENCE
FOR WEIGHT MATRIX : landsat_thies.gal
(row-standardized weights)
TEST      MI/DF      VALUE      PROB
Moran's I (error)      0.501118  6.4968261  0.0000000
Lagrange Multiplier (lag)      1      24.6219184  0.0000007
Robust LM (lag)      1      0.0788431  0.7788714
Lagrange Multiplier (error)      1      32.1432699  0.0000000
Robust LM (error)      1      7.6001945  0.0058362
Lagrange Multiplier (SARMA)      2      32.2221129  0.0000001
===== END OF REPORT =====
    
```

Spatial error model between *lnBiom\_f* and Landsat derived *lnRVI* for all sites.

```

Spatial Regression
SUMMARY OF OUTPUT: SPATIAL ERROR MODEL - MAXIMUM LIKELIHOOD ESTIMATION
Data set          : landsat_thies
Spatial weight    : landsat_thies.gal
Dependent Variable : lnBiom_f      Number of Observations: 57
Mean dependent var : 4.399470    Number of Variables   : 2
S.D. dependent var : 0.626251    Degrees of Freedom    : 55
Lag coeff. (Lambda) : 0.732502
  
```

```

R-squared          : 0.794590    R-squared (BUSE)      : -
Sq. Correlation    : -          Log likelihood         : -13.768380
Sigma-square       : 0.0805597  Akaike info criterion : 31.5368
S.E of regression  : 0.28383    Schwarz criterion     : 35.6229
  
```

Variable	Coefficient	Std. Error	z-value	Probability
CONSTANT	3.420513	0.2156528	15.8612	0.0000000
LNR	0.8876216	0.1476782	6.010514	0.0000000
LAMBDA	0.7325023	0.09064533	8.080971	0.0000000

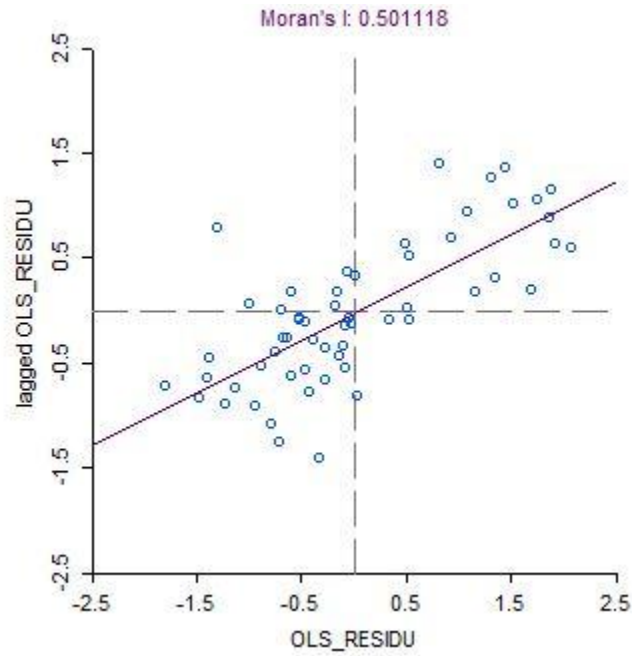
```

REGRESSION DIAGNOSTICS
DIAGNOSTICS FOR HETEROSKEDASTICITY
RANDOM COEFFICIENTS
TEST          DF      VALUE      PROB
Breusch-Pagan test    1      3.128823  0.0769193
  
```

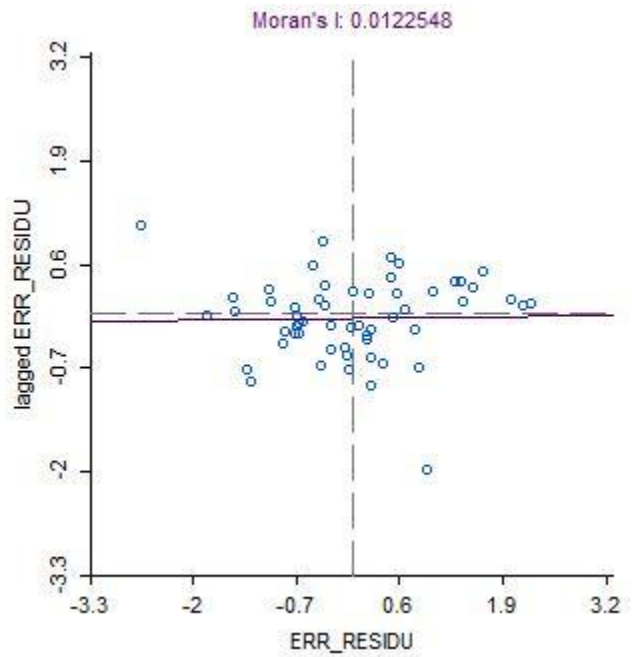
```

DIAGNOSTICS FOR SPATIAL DEPENDENCE
SPATIAL ERROR DEPENDENCE FOR WEIGHT MATRIX : landsat_thies.gal
TEST          DF      VALUE      PROB
Likelihood Ratio Test  1      28.3351  0.0000001
===== END OF REPORT =====
  
```

Moran's I of (a) classic linear regression between  $\ln Biom_f$  and Landsat derived  $\ln RVI$  for all sites; (b) spatial error model between  $\ln Biom_f$  and Landsat derived  $\ln RVI$  for all sites.



(a)



(b)

Classic linear regression between *lnBiod* and Landsat derived *RVI* for all sites.

```

Regression
SUMMARY OF OUTPUT: ORDINARY LEAST SQUARES ESTIMATION
Data set      : landsat_thies
Dependent variable : lnBiod   Number of Observations: 57
Mean dependent var : 3.217   Number of Variables : 2
S.D. dependent var : 0.478358 Degrees of Freedom : 55

R-squared      : 0.609051   F-statistic      : 85.6832
Adjusted R-squared : 0.601943   Prob(F-statistic) : 8.24144e-013
Sum squared residual: 5.0992   Log likelihood   : -12.0814
Sigma-square    : 0.0927127 Akaike info criterion : 28.1628
S.E. of regression : 0.304488   Schwarz criterion : 32.2489
Sigma-square ML : 0.0894596
S.E. of regression ML: 0.299098
  
```

Variable	Coefficient	Std. Error	t-Statistic	Probability
CONSTANT	2.51567	0.08583172	29.30932	0.0000000
RVI	0.1955183	0.02112222	9.256524	0.0000000

```

REGRESSION DIAGNOSTICS
MULTICOLLINEARITY CONDITION NUMBER 4.006860
(Extreme Multicollinearity)TEST ON NORMALITY OF ERRORS
TEST      DF      VALUE      PROB
Jarque-Bera 2      2.467262  0.2912332
  
```

```

DIAGNOSTICS FOR HETEROSKEDASTICITY
RANDOM COEFFICIENTS
TEST      DF      VALUE      PROB
Breusch-Pagan test 1      0.03103145  0.8601703
Koenker-Bassett test 1      0.05600129  0.8129315
SPECIFICATION ROBUST TEST
TEST      DF      VALUE      PROB
white 2      2.002564  0.3674081
  
```

```

DIAGNOSTICS FOR SPATIAL DEPENDENCE
FOR WEIGHT MATRIX : landsat_thies.gal
(row-standardized weights)
TEST      MI/DF      VALUE      PROB
Moran's I (error) 0.433430  5.6337578  0.0000000
Lagrange Multiplier (lag) 1      21.0332266  0.0000045
Robust LM (lag) 1      1.1609586  0.2812668
Lagrange Multiplier (error) 1      24.0462236  0.0000009
Robust LM (error) 1      4.1739556  0.0410499
Lagrange Multiplier (SARMA) 2      25.2071822  0.0000034
===== END OF REPORT =====
  
```

Spatial error model between *lnBiod* and Landsat derived *RVI* for all sites.

```
Spatial Regression
SUMMARY OF OUTPUT: SPATIAL ERROR MODEL - MAXIMUM LIKELIHOOD ESTIMATION
Data set          : landsat_thies
Spatial weight    : landsat_thies.gal
Dependent variable : lnBiod      Number of Observations: 57
Mean dependent var : 3.217003   Number of Variables   : 2
S.D. dependent var : 0.478358   Degrees of Freedom    : 55
Lag coeff. (Lambda) : 0.683372
```

```
R-squared          : 0.767229   R-squared (BUSE)      : -
Sq. Correlation    : -          Log likelihood        : -1.184318
Sigma-square       : 0.0532641 Akaike info criterion : 6.36864
S.E of regression  : 0.23079   Schwarz criterion     : 10.4547
```

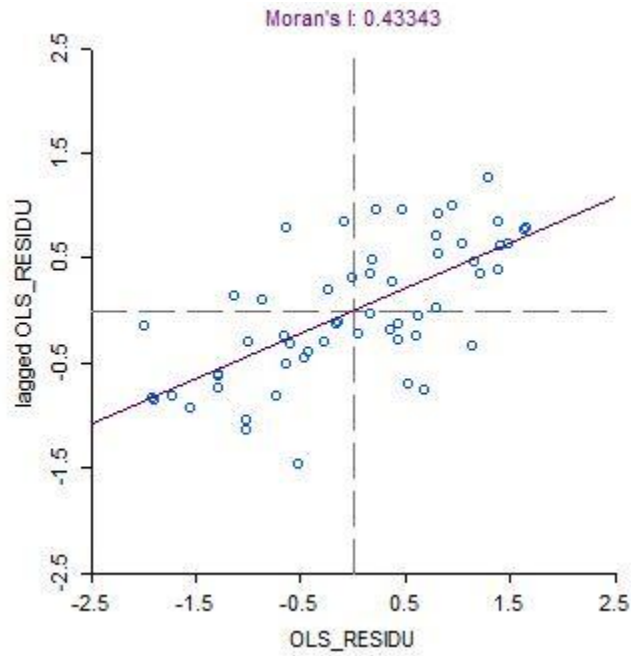
variable	Coefficient	Std.Error	z-value	Probability
CONSTANT	2.59828	0.1380855	18.81645	0.0000000
RVI	0.1728578	0.02772182	6.235444	0.0000000
LAMBDA	0.6833723	0.102087	6.69402	0.0000000

```
REGRESSION DIAGNOSTICS
DIAGNOSTICS FOR HETEROSKEDASTICITY
RANDOM COEFFICIENTS
TEST          DF      VALUE      PROB
Breusch-Pagan test      1      0.04459141  0.8327571
```

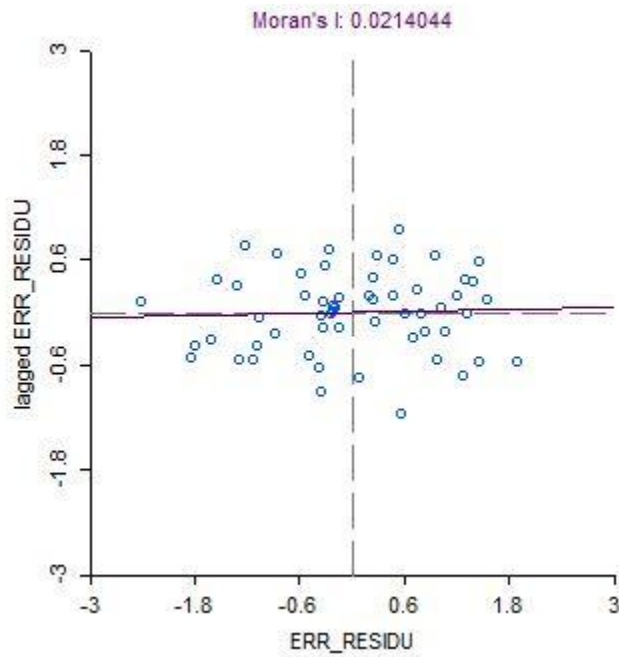
```
DIAGNOSTICS FOR SPATIAL DEPENDENCE
SPATIAL ERROR DEPENDENCE FOR WEIGHT MATRIX : landsat_thies.gal
TEST          DF      VALUE      PROB
Likelihood Ratio Test    1      21.79418  0.0000030
===== END OF REPORT =====
```



Moran's I of (a) classic linear regression between *lnBiod* and Landsat derived *RVI* for all sites; (b) spatial error model between *lnBiod* and Landsat derived *RVI* for all sites.



(a)



(b)

Classic linear regression between *lnBiom<sub>f</sub>* and Landsat derived *lnNDVI* for meadow sites.

```

Regression
SUMMARY OF OUTPUT: ORDINARY LEAST SQUARES ESTIMATION
Data set      : m_l_th
Dependent variable : lnBiom_f   Number of Observations: 30
Mean dependent var : 4.72496   Number of Variables   : 2
S.D. dependent var : 0.3831    Degrees of Freedom    : 28

R-squared      : 0.488354   F-statistic           : 26.7253
Adjusted R-squared : 0.470081   Prob(F-statistic)    : 1.74421e-005
Sum squared residual: 2.25276   Log likelihood        : -3.73253
Sigma-square    : 0.0804557 Akaike info criterion : 11.4651
S.E. of regression : 0.283647   Schwarz criterion     : 14.2675
Sigma-square ML  : 0.075092
S.E. of regression ML: 0.274029
  
```

variable	Coefficient	Std. Error	t-Statistic	Probability
CONSTANT	5.721551	0.1996118	28.66339	0.0000000
lnNDVI	2.260352	0.4372348	5.169653	0.0000174

```

REGRESSION DIAGNOSTICS
MULTICOLLINEARITY CONDITION NUMBER 7.577029
(Extreme Multicollinearity)TEST ON NORMALITY OF ERRORS
TEST      DF      VALUE      PROB
Jarque-Bera 2      1.253542  0.5343144
  
```

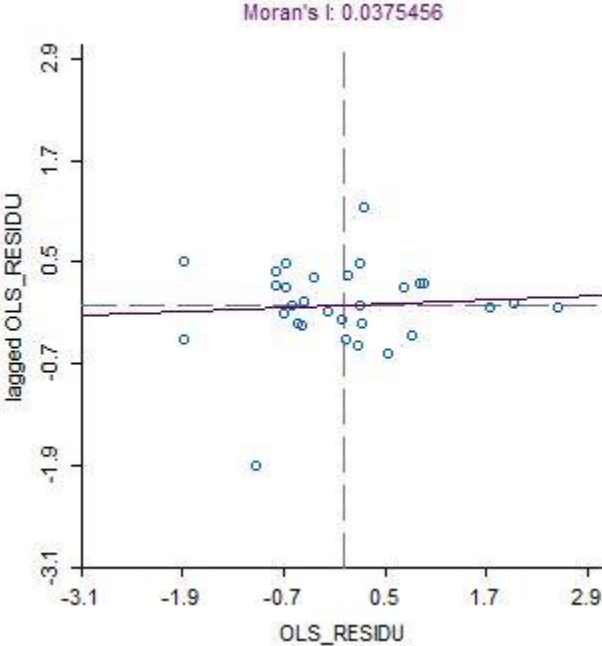
```

DIAGNOSTICS FOR HETEROSKEDASTICITY
RANDOM COEFFICIENTS
TEST      DF      VALUE      PROB
Breusch-Pagan test 1      0.07066727  0.7903677
Koenker-Bassett test 1      0.05755639  0.8104007
SPECIFICATION ROBUST TEST
TEST      DF      VALUE      PROB
white     2      4.905434   0.0860594
  
```

```

DIAGNOSTICS FOR SPATIAL DEPENDENCE
FOR WEIGHT MATRIX : m_l_th.gwt
(row-standardized weights)
TEST      MI/DF      VALUE      PROB
Moran's I (error) 0.037546  0.6914660  0.4892726
Lagrange Multiplier (lag) 1      0.0447893  0.8323919
Robust LM (lag) 1      0.0819875  0.7746219
Lagrange Multiplier (error) 1      0.0874844  0.7673999
Robust LM (error) 1      0.1246826  0.7240103
Lagrange Multiplier (SARMA) 2      0.1694719  0.9187549
===== END OF REPORT =====
  
```

Moran's I of classic linear regression between  $\ln\text{Biom}_f$  and Landsat derived  $\ln\text{NDVI}$  for meadow sites.



Classic linear regression between *lnBiod* and Landsat-derived *MSAVI* for meadow sites.

```

Regression
SUMMARY OF OUTPUT: ORDINARY LEAST SQUARES ESTIMATION
Data set      : m_L_th
Dependent variable : lnBiod   Number of Observations: 30
Mean dependent var : 3.5667   Number of Variables : 2
S.D. dependent var : 0.322228  Degrees of Freedom : 28

R-squared      : 0.306227  F-statistic      : 12.359
Adjusted R-squared : 0.281450  Prob(F-statistic) : 0.00151399
Sum squared residual: 2.16105   Log likelihood    : -3.10909
Sigma-square    : 0.0771803 Akaike info criterion : 10.2182
S.E. of regression : 0.277813   Schwarz criterion  : 13.0206
Sigma-square ML  : 0.0720349
S.E. of regression ML: 0.268393

-----
Variable      Coefficient      Std. Error      t-Statistic      Probability
-----
CONSTANT      2.778482         0.2298758      12.08688         0.0000000
MSAVI         2.262227         0.6434933      3.515541         0.0015140
-----

REGRESSION DIAGNOSTICS
MULTICOLLINEARITY CONDITION NUMBER 8.952527
TEST ON NORMALITY OF ERRORS
TEST      DF      VALUE      PROB
Jarque-Bera      2      4.019678      0.1340103

DIAGNOSTICS FOR HETEROSKEDASTICITY
RANDOM COEFFICIENTS
TEST      DF      VALUE      PROB
Breusch-Pagan test      1      2.275839      0.1314040
Koenker-Bassett test    1      1.751811      0.1856493
SPECIFICATION ROBUST TEST
TEST      DF      VALUE      PROB
white      2      2.639976      0.2671385

DIAGNOSTICS FOR SPATIAL DEPENDENCE
FOR WEIGHT MATRIX : m_L_th.gwt
(row-standardized weights)
TEST      MI/DF      VALUE      PROB
Moran's I (error)      0.441372      4.2574566      0.0000207
Lagrange Multiplier (lag)      1      0.0891354      0.7652792
Robust LM (lag)      1      0.5183957      0.4715268
Lagrange Multiplier (error)      1      12.0898903      0.0005070
Robust LM (error)      1      12.5191506      0.0004028
Lagrange Multiplier (SARMA)      2      12.6082860      0.0018287
===== END OF REPORT =====

```

Spatial error model between *lnBiod* and Landsat-derived *MSAVI* for meadow sites.

```
Spatial Regression
SUMMARY OF OUTPUT: SPATIAL ERROR MODEL - MAXIMUM LIKELIHOOD ESTIMATION
Data set          : m_L_th
Spatial weight    : m_L_th.gwt
Dependent Variable : lnBiod      Number of Observations: 30
Mean dependent var : 3.566703   Number of Variables   : 2
S.D. dependent var : 0.322228   Degrees of Freedom    : 28
Lag coeff. (Lambda) : 0.759146
```

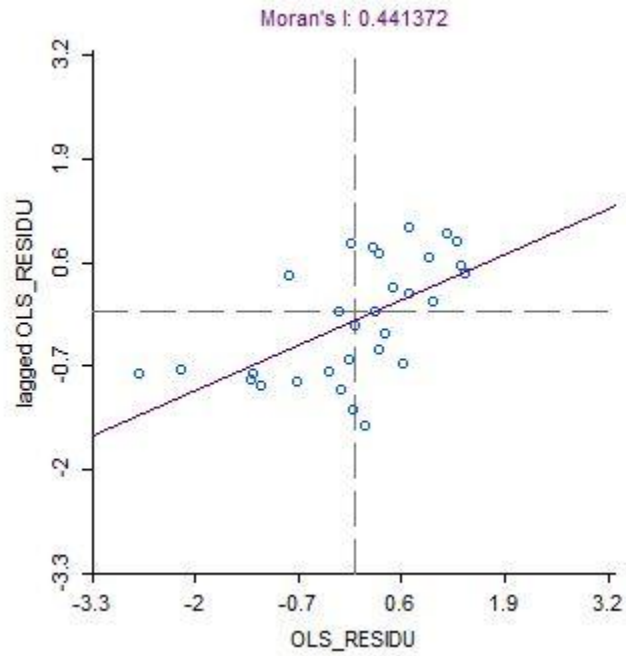
```
R-squared          : 0.679674   R-squared (BUSE)      : -
Sq. Correlation    : -          Log likelihood        : 5.442037
Sigma-square       : 0.0332597  Akaike info criterion : -6.88407
S.E of regression  : 0.182372   Schwarz criterion     : -4.08168
```

Variable	Coefficient	Std. Error	z-value	Probability
CONSTANT	2.329547	0.1898879	12.26801	0.0000000
MSAVI	3.894858	0.4658781	8.360252	0.0000000
LAMBDA	0.759146	0.1029396	7.374673	0.0000000

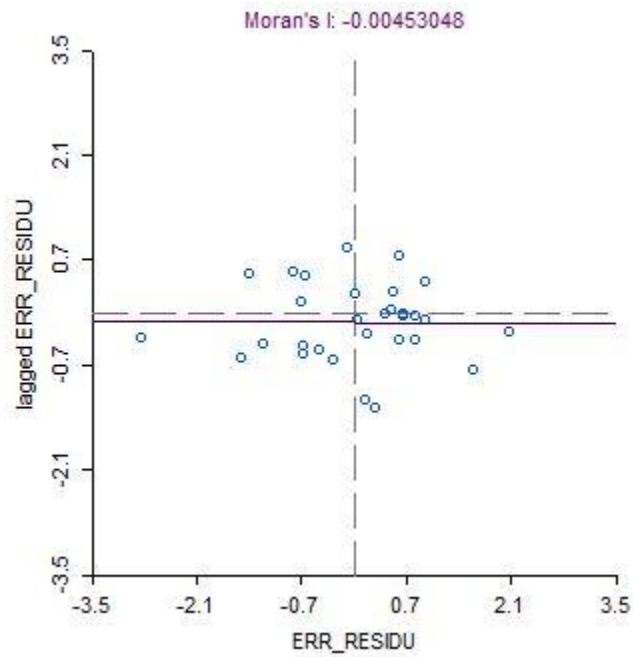
```
REGRESSION DIAGNOSTICS
DIAGNOSTICS FOR HETEROSKEDASTICITY
RANDOM COEFFICIENTS
TEST          DF      VALUE      PROB
Breusch-Pagan test  1      2.626365  0.1051021
```

```
DIAGNOSTICS FOR SPATIAL DEPENDENCE
SPATIAL ERROR DEPENDENCE FOR WEIGHT MATRIX : m_L_th.gwt
TEST          DF      VALUE      PROB
Likelihood Ratio Test  1      17.10225  0.0000354
===== END OF REPORT =====
```

Moran's I of (a) classic linear regression between *lnBiod* and Landsat derived *MSAVI* for all sites; (b) spatial error model between *lnBiod* and Landsat derived *MSAVI* for all sites.



(a)



(b)

Classic linear regression between *lnBiom<sub>f</sub>* and hyper *NDVI* for all sites.

```

Regression
SUMMARY OF OUTPUT: ORDINARY LEAST SQUARES ESTIMATION
Data set      : hyper_thies
Dependent variable : lnBiom_f      Number of Observations: 57
Mean dependent var : 4.39947      Number of Variables   : 2
S.D. dependent var : 0.626251      Degrees of Freedom    : 55

R-squared      : 0.760532      F-statistic           : 174.676
Adjusted R-squared : 0.756178      Prob(F-statistic)    : 1.03795e-018
Sum squared residual: 5.35327      Log likelihood        : -13.4672
Sigma-square    : 0.0973322     Akaike info criterion : 30.9344
S.E. of regression : 0.311981      Schwarz criterion     : 35.0205
Sigma-square ML  : 0.093917
S.E. of regression ML: 0.306459
  
```

variable	Coefficient	Std. Error	t-Statistic	Probability
CONSTANT	3.070134	0.1087393	28.23389	0.0000000
NDVI	2.730182	0.206574	13.21649	0.0000000

```

REGRESSION DIAGNOSTICS
MULTICOLLINEARITY CONDITION NUMBER 5.065495
(Extreme Multicollinearity)TEST ON NORMALITY OF ERRORS
TEST      DF      VALUE      PROB
Jarque-Bera      2      1.201958      0.5482745
  
```

```

DIAGNOSTICS FOR HETEROSKEDASTICITY
RANDOM COEFFICIENTS
TEST      DF      VALUE      PROB
Breusch-Pagan test      1      0.3908739      0.5318404
Koenker-Bassett test    1      0.5869247      0.4436108
SPECIFICATION ROBUST TEST
TEST      DF      VALUE      PROB
white      2      4.285541      0.1173293
  
```

```

DIAGNOSTICS FOR SPATIAL DEPENDENCE
FOR WEIGHT MATRIX : hyper_thies.gal
(row-standardized weights)
TEST      MI/DF      VALUE      PROB
Moran's I (error)      0.274317      3.7366271      0.0001866
Lagrange Multiplier (lag)      1      5.7123858      0.0168456
Robust LM (lag)      1      0.0036843      0.9515996
Lagrange Multiplier (error)      1      9.6319917      0.0019122
Robust LM (error)      1      3.9232902      0.0476216
Lagrange Multiplier (SARMA)      2      9.6356760      0.0080842
===== END OF REPORT =====
  
```

Spatial error model between *lnBiom\_f* and hyper *NDVI* for all sites.

```

Spatial Regression
SUMMARY OF OUTPUT: SPATIAL ERROR MODEL - MAXIMUM LIKELIHOOD ESTIMATION
Data set          : hyper_thies
Spatial weight    : hyper_thies.gal
Dependent variable : lnBiom_f      Number of Observations: 57
Mean dependent var : 4.399470     Number of Variables   : 2
S.D. dependent var : 0.626251     Degrees of Freedom    : 55
Lag coeff. (Lambda) : 0.464360
  
```

```

R-squared          : 0.803007   R-squared (BUSE)      : -
Sq. Correlation    : -          Log likelihood         : -9.440294
Sigma-square       : 0.0772588 Akaike info criterion : 22.8806
S.E of regression  : 0.277955   Schwarz criterion     : 26.9667
  
```

Variable	Coefficient	Std. Error	z-value	Probability
CONSTANT	3.080003	0.1580157	19.49175	0.0000000
NDVI	2.718435	0.2928484	9.282739	0.0000000
LAMBDA	0.4643597	0.1444224	3.215289	0.0013033

```

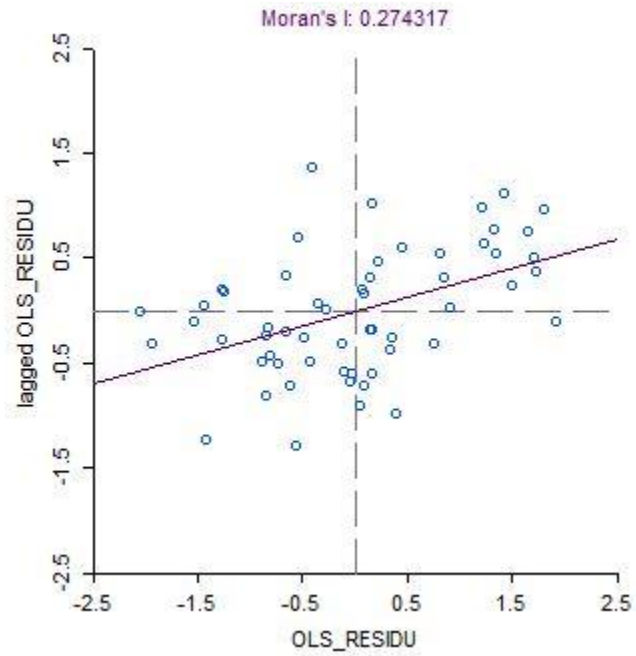
REGRESSION DIAGNOSTICS
DIAGNOSTICS FOR HETEROSKEDASTICITY
RANDOM COEFFICIENTS
TEST          DF      VALUE      PROB
Breusch-Pagan test  1      0.4709235  0.4925626
  
```

```

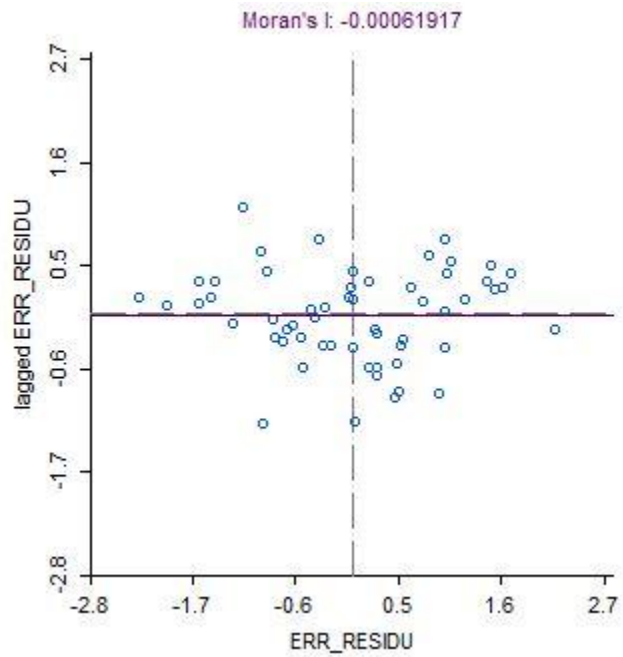
DIAGNOSTICS FOR SPATIAL DEPENDENCE
SPATIAL ERROR DEPENDENCE FOR WEIGHT MATRIX : hyper_thies.gal
TEST          DF      VALUE      PROB
Likelihood Ratio Test  1      8.053816  0.0045408
===== END OF REPORT =====
  
```



Moran's I of (a) classic linear regression between  $\ln Biom\_f$  and hyper  $NDVI$  for all sites; (b) spatial error model between  $\ln Biom\_f$  and hyper  $NDVI$  for all sites.



(a)



(b)

Classic linear regression between *lnBiod* and hyper *MSAVI* for all sites.

```

Regression
SUMMARY OF OUTPUT: ORDINARY LEAST SQUARES ESTIMATION
Data set      : hyper_thies
Dependent variable : lnBiod      Number of Observations: 57
Mean dependent var : 3.217      Number of Variables : 2
S.D. dependent var : 0.478358    Degrees of Freedom : 55

R-squared      : 0.587980    F-statistic      : 78.4888
Adjusted R-squared : 0.580489    Prob(F-statistic) : 3.54939e-012
Sum squared residual: 5.37402    Log likelihood   : -13.5775
Sigma-square    : 0.0977095   Akaike info criterion : 31.1549
S.E. of regression : 0.312585    Schwarz criterion : 35.241
Sigma-square ML  : 0.0942811
S.E. of regression ML: 0.307052

-----
Variable      Coefficient      Std. Error      t-Statistic      Probability
-----
CONSTANT      2.34631          0.1066442      22.00128         0.0000000
MSAVI         2.99527          0.3380898      8.859391         0.0000000
-----

REGRESSION DIAGNOSTICS
MULTICOLLINEARITY CONDITION NUMBER 4.949492
(Extreme Multicollinearity)TEST ON NORMALITY OF ERRORS
TEST      DF      VALUE      PROB
Jarque-Bera      2      2.578605      0.2754629

DIAGNOSTICS FOR HETEROSKEDASTICITY
RANDOM COEFFICIENTS
TEST      DF      VALUE      PROB
Breusch-Pagan test      1      0.5909851      0.4420385
Koenker-Bassett test    1      0.6180383      0.4317772
SPECIFICATION ROBUST TEST
TEST      DF      VALUE      PROB
white      2      2.901402      0.2344060

DIAGNOSTICS FOR SPATIAL DEPENDENCE
FOR WEIGHT MATRIX : hyper_thies.gal
(row-standardized weights)
TEST      MI/DF      VALUE      PROB
Moran's I (error)      0.313720      4.1604641      0.0000318
Lagrange Multiplier (lag)      1      18.6200385      0.0000160
Robust LM (lag)      1      6.0505348      0.0139021
Lagrange Multiplier (error)      1      12.5977562      0.0003862
Robust LM (error)      1      0.0282525      0.8665165
Lagrange Multiplier (SARMA)      2      18.6482910      0.0000892
===== END OF REPORT =====

```

Spatial error model between *lnBiod* and hyper *MSAVI* for all sites.

```

Spatial Regression
SUMMARY OF OUTPUT: SPATIAL LAG MODEL - MAXIMUM LIKELIHOOD ESTIMATION
Data set          : hyper_thies
Spatial weight    : hyper_thies.gal
Dependent variable : lnBiod| Number of Observations: 57
Mean dependent var : 3.217 Number of Variables : 3
S.D. dependent var : 0.478358 Degrees of Freedom : 54
Lag coeff. (Rho)  : 0.53975
  
```

```

R-squared          : 0.719218 Log likelihood      : -4.82051
Sq. Correlation    : - Akaike info criterion : 15.641
Sigma-square       : 0.0642504 Schwarz criterion : 21.7702
S.E of regression  : 0.253477
  
```

Variable	Coefficient	Std. Error	z-value	Probability
W_LNBIOD	0.5397502	0.1077819	5.0078	0.0000006
CONSTANT	0.988274	0.2868132	3.445706	0.0005697
MSAVI	1.691043	0.3704939	4.564294	0.0000050

REGRESSION DIAGNOSTICS  
 DIAGNOSTICS FOR HETEROSKEDASTICITY  
 RANDOM COEFFICIENTS

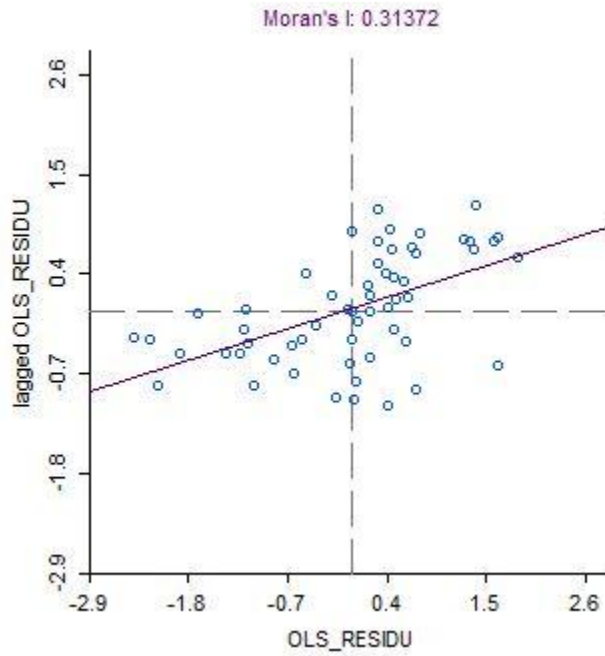
TEST	DF	VALUE	PROB
Breusch-Pagan test	1	0.275799	0.5994680

DIAGNOSTICS FOR SPATIAL DEPENDENCE  
 SPATIAL LAG DEPENDENCE FOR WEIGHT MATRIX : hyper\_thies.gal

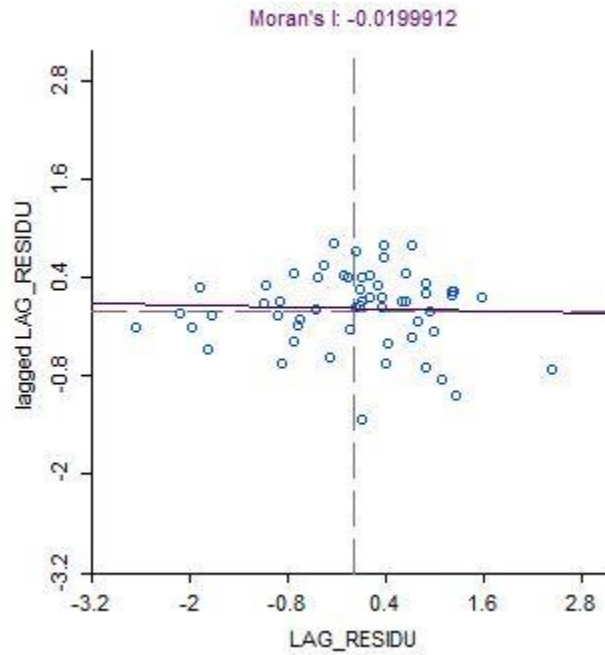
TEST	DF	VALUE	PROB
Likelihood Ratio Test	1	17.5139	0.0000285

===== END OF REPORT =====

Moran's I of (a) classic linear regression between *lnBiod* and hyper *MSAVI* for all sites; (b) spatial lag model between *lnBiod* and hyper *MSAVI* for all sites.



(a)



(b)

Classic linear regression between *lnBiom<sub>f</sub>* and hyper *lnNDVI* for meadow sites.

```

Regression
SUMMARY OF OUTPUT: ORDINARY LEAST SQUARES ESTIMATION
Data set      : m_h_th
Dependent variable : lnBiom_f  Number of Observations: 30
Mean dependent var : 4.72496  Number of Variables   : 2
S.D. dependent var : 0.3831   Degrees of Freedom    : 28

R-squared      : 0.360324  F-statistic          : 15.7722
Adjusted R-squared : 0.337478  Prob(F-statistic)   : 0.000453654
Sum squared residual: 2.81647  Log likelihood      : -7.08246
Sigma-square    : 0.100588  Akaike info criterion : 18.1649
S.E. of regression : 0.317156  Schwarz criterion   : 20.9673
Sigma-square ML  : 0.0938823
S.E. of regression ML: 0.306402
  
```

Variable	Coefficient	Std. Error	t-Statistic	Probability
CONSTANT	5.439052	0.1889014	28.79307	0.0000000
lnNDVI	1.521905	0.3832147	3.971417	0.0004537

```

REGRESSION DIAGNOSTICS
MULTICOLLINEARITY CONDITION NUMBER 6.367528
(Extreme Multicollinearity)TEST ON NORMALITY OF ERRORS
TEST      DF      VALUE      PROB
Jarque-Bera 2      0.5206971  0.7707829
  
```

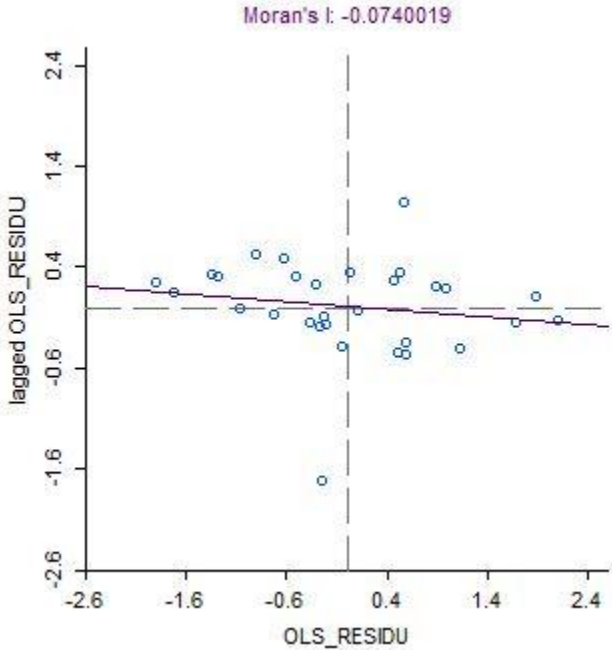
```

DIAGNOSTICS FOR HETEROSKEDASTICITY
RANDOM COEFFICIENTS
TEST      DF      VALUE      PROB
Breusch-Pagan test 1      0.06439064  0.7996863
Koenker-Bassett test 1      0.08068209  0.7763752
SPECIFICATION ROBUST TEST
TEST      DF      VALUE      PROB
white 2      6.574578  0.0373550
  
```

```

DIAGNOSTICS FOR SPATIAL DEPENDENCE
FOR WEIGHT MATRIX : m_h_th.gwt
(row-standardized weights)
TEST      MI/DF      VALUE      PROB
Moran's I (error) -0.074002 -0.2460676  0.8056300
Lagrange Multiplier (lag) 1      0.8659447  0.3520804
Robust LM (lag) 1      1.2183273  0.2696892
Lagrange Multiplier (error) 1      0.3398586  0.5599109
Robust LM (error) 1      0.6922412  0.4054031
Lagrange Multiplier (SARMA) 2      1.5581859  0.4588220
===== END OF REPORT =====
  
```

Moran's I of classic linear regression between *lnBiom\_f* and hyper *lnNDVI* for meadow sites.



Classic linear regression between *lnBiod* and hyper *MSAVI* for meadow sites.

```

Regression
SUMMARY OF OUTPUT: ORDINARY LEAST SQUARES ESTIMATION
Data set      : m_h_th
Dependent variable : lnBiod      Number of Observations: 30
Mean dependent var : 3.5667      Number of Variables   : 2
S.D. dependent var : 0.322228      Degrees of Freedom    : 28

R-squared      : 0.278241      F-statistic           : 10.7941
Adjusted R-squared : 0.252464      Prob(F-statistic)    : 0.00274049
Sum squared residual: 2.24822      Log likelihood        : -3.70229
Sigma-square    : 0.0802936     Akaike info criterion : 11.4046
S.E. of regression : 0.283361      Schwarz criterion     : 14.207
Sigma-square ML  : 0.0749407
S.E. of regression ML: 0.273753
  
```

Variable	Coefficient	Std. Error	t-Statistic	Probability
CONSTANT	2.919342	0.2037177	14.33033	0.0000000
MSAVI	1.750806	0.5328985	3.285439	0.0027405

```

REGRESSION DIAGNOSTICS
MULTICOLLINEARITY CONDITION NUMBER 7.746421
(Extreme Multicollinearity)TEST ON NORMALITY OF ERRORS
TEST      DF      VALUE      PROB
Jarque-Bera      2      6.294161      0.0429774
  
```

```

DIAGNOSTICS FOR HETEROSKEDASTICITY
RANDOM COEFFICIENTS
TEST      DF      VALUE      PROB
Breusch-Pagan test      1      0.1868543      0.6655477
Koenker-Bassett test    1      0.1212401      0.7276933
SPECIFICATION ROBUST TEST
TEST      DF      VALUE      PROB
white      2      0.4028731      0.8175555
  
```

```

DIAGNOSTICS FOR SPATIAL DEPENDENCE
FOR WEIGHT MATRIX : m_h_th.gwt
(row-standardized weights)
TEST      MI/DF      VALUE      PROB
Moran's I (error)      0.343826      3.3067708      0.0009439
Lagrange Multiplier (lag)      1      0.4227516      0.5155672
Robust LM (lag)      1      0.0155524      0.9007536
Lagrange Multiplier (error)      1      7.3365246      0.0067567
Robust LM (error)      1      6.9293254      0.0084794
Lagrange Multiplier (SARMA)      2      7.3520770      0.0253231
===== END OF REPORT =====
  
```

Spatial error model between *lnBiod* and hyper *MSAVI* for meadow sites.

```

Spatial Regression
SUMMARY OF OUTPUT: SPATIAL ERROR MODEL - MAXIMUM LIKELIHOOD ESTIMATION
Data set          : m_h_th
Spatial weight    : m_h_th.gwt
Dependent Variable : lnBiod      Number of Observations: 30
Mean dependent var : 3.566703   Number of variables   : 2
S.D. dependent var : 0.322228   Degrees of Freedom    : 28
Lag coeff. (Lambda) : 0.533478
  
```

```

|
R-squared          : 0.472234   R-squared (BUSE)      : -
Sq. Correlation    : -          Log likelihood         : -0.221444
Sigma-square       : 0.0547983  Akaike info criterion : 4.44289
S.E of regression  : 0.23409   Schwarz criterion     : 7.24528
  
```

Variable	Coefficient	Std.Error	z-value	Probability
CONSTANT	2.689047	0.1933816	13.90539	0.0000000
MSAVI	2.452489	0.4665957	5.256133	0.0000001
LAMBDA	0.5334778	0.1696761	3.144094	0.0016662

REGRESSION DIAGNOSTICS  
 DIAGNOSTICS FOR HETEROSKEDASTICITY  
 RANDOM COEFFICIENTS

TEST	DF	VALUE	PROB
Breusch-Pagan test	1	0.3380662	0.5609476

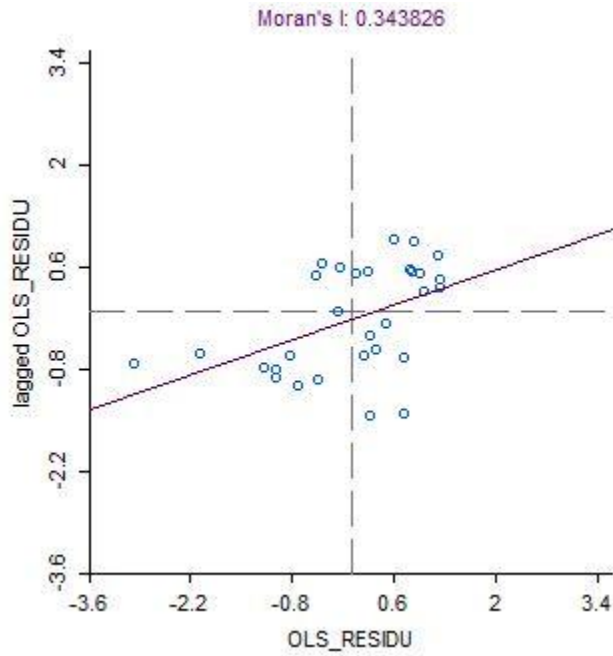
DIAGNOSTICS FOR SPATIAL DEPENDENCE

TEST	DF	VALUE	PROB
Likelihood Ratio Test	1	6.961692	0.0083273

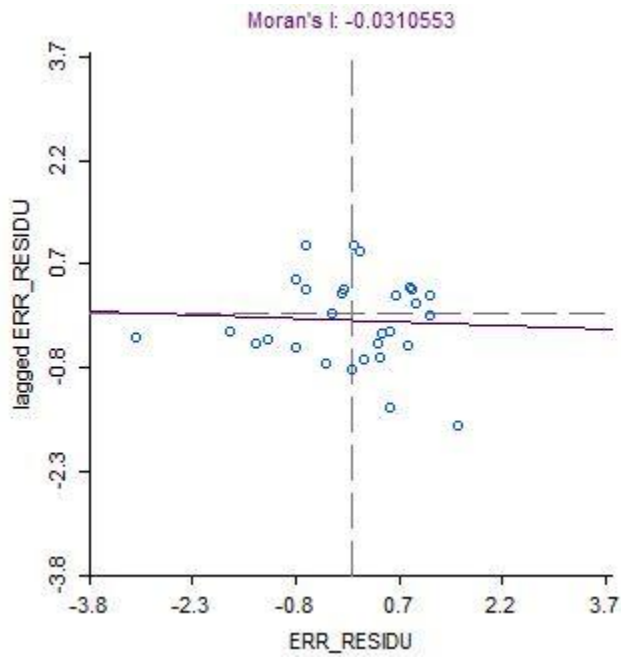
===== END OF REPORT =====



Moran's I of (a) classic linear regression between *lnBiod* and hyper *MSAVI* for all sites; (b) spatial error model between *lnBiod* and hyper *MSAVI* for meadow sites.



(a)



(b)

## Citations

- Akaike, H. (1974). A new look at the statistical model identification. *IEEE Transactions on Automatic Control*, 19 (6), 716-723.
- Anderson, G.L., Hanson, J.D., Haas, R.H. (1993). Evaluating Landsat Thematic mapper derived vegetation indices for estimating aboveground biomass on semiarid rangelands. *Remote Sensing of Environment*, 45, 165-175
- Anselin, L. (1988). *Spatial Econometrics: Methods and Models*. Dordrecht, the Netherlands: Klumer.
- Anselin, L. (2005). *Exploring Spatial Data with GeoDa: A Workbook*. Spatial Analysis Laboratory, Department of Geography, University of Illinois, Urbana-Champaign. USA: Urbana.
- Bai, Y., Wu, J., Xing, Q., Pan, Q., Huang, J., Yang, D., and Han, X. (2008). Primary production and rain use efficiency across a precipitation gradient on the Mongolia Plateau. *Ecology*, 89(8), 2140-2153.
- Baret F. & Guyot, G. (1991). TSAVI: a vegetation index which minimizes soil brightness effects on LAI and APAR estimation. *Remote Sensing of Environment*, 35, 161-173.
- Chapin, F.S., Sala, O.E., Huber-Sannwald, E. (2001). *Global Biodiversity in a Changing Environment : Scenarios for the 21<sup>st</sup> Century*. Springer-Verlag, New York, USA.
- Cho, M.A., Skidmore, A., Corsi, F., van Wieren, S.E., Sobhan, I. (2007). Estimation of green grass/herb biomass from airborne hyperspectral imagery using spectral indices and partial least squares regression. *International Journal of Applied Earth Observation and Geoinformation*, 9, 414-424.
- Du, Y., Chang, C., Ren, H., Chang, C., Jensen, J.O. (2004). New hyperspectral discrimination measure for spectral characterization. *Society of Photo-Optical Instrumentation Engineers*. 43(8), 1777-1786.
- Gao, X., Chen, Y., Lu, S., Feng, C., Chang, X., Ye, S., and Liu, J. (2012). A ground spectral model for estimating biomass at the peak of the growing season in Hulunbeier grassland, Inner Mongolia, China. *International Journal of Remote Sensing*, Vol. 33, No. 13, 4029-4043
- Gillespie, T.W., Saatchi, S., Pau, S., Bohlman, S., Giorgi, A.P., Lewis, S. (2009). Towards quantifying tropical tree species richness in tropical forests. *International Journal of Remote Sensing*, Vol. 30, No. 6, 1629-1634.
- Gould, W. (2000). Remote sensing of vegetation, plant species richness, and regional biodiversity hotspots. *Ecological Society of America*, 10(6), 1861-1870.
- He, C., Zhang, Q., Li, Y., Li, X., Shi, P. (2005). Zoning grassland protection area using remote sensing and cellular automata modeling-a case study in Xilingol steppe grassland in northern China. *International Journal of Remote Sensing*, 25, 1723-1732

- Huete, A.R. (1988). A soil-adjusted vegetation index (SAVI). *Remote Sensing of Environment*, 25, 295-309.
- Jiang, G., Han, X., Wu, J. (2006). Restoration and management of the Inner Mongolia grassland require a sustainable strategy. *Ambio*, 35, 269–270.
- Kawamura, K., Akiyama, T., Yokot, H., Tsutsumi, M., Yasuda, T., Watanabe, O., Wang, S. (2005). Quantifying grazing intensities using geographic information systems and satellite remote sensing in the Xilingol steppe region, Inner Mongolia, China. *Agriculture, Ecosystems and Environment*, 107, 83-93.
- Li, R., Liu, Y. (2001) An estimation of wetland vegetation biomass in the Poyang lake using Landsat ETM data. *Acta Geographica Sinica*, 56, 532-540
- Moore, C.W.E. (1966). Distribution of grasslands. In: Barnard, C. (Ed.), *Grasses and Grasslands*. Macmillan, New York, pp. 182-205.
- Mutanga, O. (2004). Hyperspectral remote sensing of tropical grass quality and quantity. Ph.D. Dissertation. Wageningen University, Wageningen, The Netherlands.
- Mutanga, O., Skidmore, A. (2004). Narrow band vegetation indices overcome the saturation problem in biomass estimation. *International Journal of Remote Sensing*, 25, 1-16.
- Nagendra, H. (2001). Using remote sensing to assess biodiversity. *International Journal of Remote Sensing*, Vol. 22, No. 12, 2377-2400.
- Nagendra, H., Rocchini, D. (2008). High resolution satellite imagery for tropical biodiversity studies: the devil is in the detail. *Biodiversity Conservation*, 17, 3431-3442.
- Palmer M.W., Earls, P.G., Hoagland, B.W., White, P.S., Wohlgemuth, T. (2002). Quantitative tools for perfecting species lists. *Enviornmetrics*, 13, 121-137.
- Parviainen, M., Luoto, M., Heikkinen, R.K. (2009). The role of local and landscape level measures of greenness in modeling boreal plant species richness. *Ecological Modeling*, 220, 2690-2701.

- Qi, J., Chehbouni, A., Huete, A.R., Kerr, Y.H., Sorooshian, S. (1994). A modified soil adjusted vegetation index. *Remote Sensing of Environment*, 48, 119-126
- Qi, X., Ji, M., Meng, H. (2008). *An Illustrated Handbook on Habitual Plant of Inner Mongolia Grassland*. Hohhot, Inner Mongolia, China.
- Ren, A. (2008). Grassland biomass on north-western plateau of Sichun and vegetation indexes relation using Landsat TM image. Master Thesis. Sichuan Agricultural University, Ya'an, China. (in Chinese, with English abstract).
- Ren, H., Zhou, G., Zhang, X. (2011). Estimation of green aboveground biomass of desert steppe in Inner Mongolia based on red-edge reflectance curve area method. *Biosystems Engineering*, 109, 385-395.
- Ricklefs, R.E. (2010). *The Economy of Nature*. New York, USA.
- Rocchini, D. (2007). Effects of spatial and spectral resolution in estimating ecosystem  $\alpha$ -diversity by satellite imagery. *Remote Sensing of Environment*, 111, 423-434.
- Rocchini, D., Ricotta, C., and Chiarucci, A. (2007). Using satellite imagery to assess plant species richness: The role of multispectral systems. *Applied Vegetation Science*. 10, 325-331.
- Tucker, C.J. (1979). Red and photographic infrared linear combinations for monitoring vegetation. *Remote Sensing of Environment*. 8, 127-150.
- Schino, G., Borfecchia, F., De Cecco, L., Dibari, C., Iannetta, M., Martini, S., Pedrotti, F. (2003). Satellite estimate of grass biomass in a mountainous range in central Italy. *Agroforestry Systems*, 59, 157-162.
- Sha, Z., Bai, Y., Xie, Y., Yu, M., Zhang, L. (2008). Using a hybrid fuzzy classifier (HFC) to map typical grassland vegetation in Xilinhe River Basin, Inner Mongolia, China. *International Journal of Remote Sensing*, 29, 2317-2337.
- Xie, Y., Sha, Z., Yu, M., Bai, Y., Zhang, L. (2009). A comparison of two models with Landsat data for estimating above ground grassland biomass in Inner Mongolia, China. *Ecological Modeling*, 220, 1810-1818.

Wang, J. (2012). People, institutions, and pixels: linking remote sensing and social science to understand social adaptation to environmental change on the Mongolian plateau. Ph.D. Dissertation. University of Michigan, Ann Arbor, USA.

Ward, M.D. & Gleditsch, K.S. 2008. *Spatial Regression Models*. Thousand Oaks, CA: Sage.

Zhang, X. (1992). Northern China. In *Grasslands and Grassland Science in Northern China*, edited by National Research Council. Washington, D.C. National Academy Press. pp: 39–54.